

2

NAVAL POSTGRADUATE SCHOOL

Monterey, California

DTIC FILE COPY

AD-A225 529



THESIS

DTIC

Aug 20 1990

COMPARISON OF THE DYNAMICS OF A LAND VS.
OCEANIC EXPLOSIVE CYCLONE.

by

Michael E. Kreyenhagen

December 1989

Thesis Advisor

W. A. Nuss

Approved for public release; distribution is unlimited.

Unclassified

security classification of this page

REPORT DOCUMENTATION PAGE

1a Report Security Classification Unclassified			1b Restrictive Markings		
2a Security Classification Authority			3 Distribution Availability of Report		
2b Declassification Downgrading Schedule			Approved for public release; distribution is unlimited.		
4 Performing Organization Report Number(s)			5 Monitoring Organization Report Number(s)		
6a Name of Performing Organization Naval Postgraduate School		6b Office Symbol (if applicable) 35	7a Name of Monitoring Organization Naval Postgraduate School		
6c Address (city, state, and ZIP code) Monterey, CA 93943-5000			7b Address (city, state, and ZIP code) Monterey, CA 93943-5000		
8a Name of Funding Sponsoring Organization		8b Office Symbol (if applicable)	9 Procurement Instrument Identification Number		
8c Address (city, state, and ZIP code)			10 Source of Funding Numbers		
			Program Element No	Project No	Task No
			Work Unit Accession No		
11 Title (include security classification) COMPARISON OF THE DYNAMICS OF A LAND VS. OCEANIC EXPLOSIVE CYCLONE.					
12 Personal Author(s) Michael E. Kreyenhagen					
13a Type of Report Master's Thesis		13b Time Covered From To		14 Date of Report (year, month, day) December 1989	
				15 Page Count	
16 Supplementary Notation The views expressed in this thesis are those of the author and do not reflect the official policy or position of the Department of Defense or the U.S. Government.					
17 Cosati Codes			18 Subject Terms (continue on reverse if necessary and identify by block number)		
Field	Group	Subgroup	Meteorology, Mid Latitude, Explosive Development, -NCS (10, 11, 12, 13, 14, 15, 16, 17, 18, 19, 20, 21, 22, 23, 24, 25, 26, 27, 28, 29, 30, 31, 32, 33, 34, 35, 36, 37, 38, 39, 40, 41, 42, 43, 44, 45, 46, 47, 48, 49, 50, 51, 52, 53, 54, 55, 56, 57, 58, 59, 60, 61, 62, 63, 64, 65, 66, 67, 68, 69, 70, 71, 72, 73, 74, 75, 76, 77, 78, 79, 80, 81, 82, 83, 84, 85, 86, 87, 88, 89, 90, 91, 92, 93, 94, 95, 96, 97, 98, 99, 100)		
19 Abstract (continue on reverse if necessary and identify by block number)					
<p>Two explosively developing cyclones are analyzed and compared using a similar diagnostic approach. A continental cyclone developed over the U.S. Mid-west during 14-17 November 1988 and was analyzed using NMC (Nested Grid model) analysis fields and GOES IR imagery. A maritime cyclone rapidly developed over the western North Atlantic Ocean during 03-05 January 1989. The NMC Spectral Model and GOES imagery are employed to describe the development of this storm. Upper-level vorticity, divergence and jet streak placement are examined along with low-level thermal advection, boundary layer heating and static stability for each storm.</p> <p>Results indicate that the land and ocean storms have similar magnitude upper-level divergence associated with 300 mb jet streaks, however, they evolve differently. At low-levels, there are equal contributions from advection and surface heating during rapid development in the ocean case while advection was the primary contribution in the land case. The initial static stability was low for both cyclones, however, the ocean case maintained low static stability and this appears to be a major factor in determining the depth and speed of rapid cyclone development.</p> <p style="text-align: right;">Keywords:</p>					
20 Distribution Availability of Abstract			21 Abstract Security Classification		
<input checked="" type="checkbox"/> unclassified unlimited <input type="checkbox"/> same as report <input type="checkbox"/> DTIC users			Unclassified		
22a Name of Responsible Individual W. A. Nuss			22b Telephone (include Area code) (408) 646-2044		22c Office Symbol 63Nu

DD FORM 1473, 84 MAR

85 APR edition may be used until exhausted
All other editions are obsolete

security classification of this page

Unclassified

Approved for public release; distribution is unlimited.

Comparison of the Dynamics of a Land vs.
Oceanic Explosive Cyclone.

by

Michael E. Kreyenhagen
Lieutenant Commander, United States Navy
B.S., United States Naval Academy, 1979

Submitted in partial fulfillment of the
requirements for the degree of

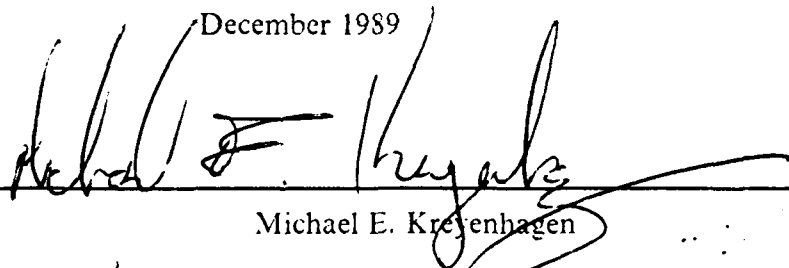
MASTER OF SCIENCE IN METEOROLOGY AND OCEANOGRAPHY

from the

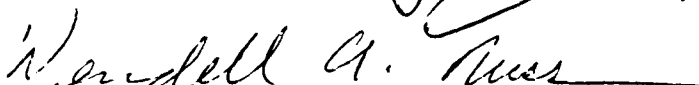
NAVAL POSTGRADUATE SCHOOL

December 1989

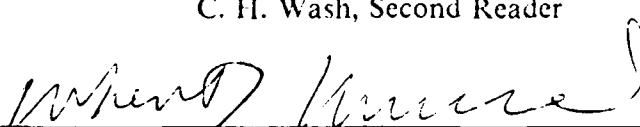
Author:


Michael E. Kreyenhagen

Approved by:


W. A. Nuss, Thesis Advisor


C. H. Wash, Second Reader


Robert J. Renard, Chairman,
Department of Meteorology

ABSTRACT.

Two explosively developing cyclones are analyzed and compared using a similar diagnostic approach. A continental cyclone developed over the U.S. Mid-west during 14-17 November 1988 and was analyzed using NMC Nested Grid model analysis fields and GOES IR imagery. A maritime cyclone rapidly developed over the western North Atlantic Ocean during 03-05 January 1989. The NMC Spectral Model and GOES imagery are employed to describe the development of this storm. Upper-level vorticity, divergence and jet streak placement are examined along with low-level thermal advection, boundary layer heating and static stability for each storm.

Results indicate that the land and ocean storms have similar magnitude upper-level divergence associated with 300 mb jet streaks, however, they evolve differently. At low-levels, there are equal contributions from advection and surface heating during rapid development in the ocean case while advection was the primary contribution in the land case. The initial static stability was low for both cyclones, however, the ocean case maintained low static stability and this appears to be a major factor in determining the depth and speed of rapid cyclone development.

Accession For	
NTIS GRA&I	<input checked="" type="checkbox"/>
DTIC TAB	<input type="checkbox"/>
Unannounced	<input type="checkbox"/>
Justification	
By	
Distribution/	
Availability Codes	
Dist	Special
A-1	



TABLE OF CONTENTS

I. INTRODUCTION.	1
A. BACKGROUND.	1
B. DESCRIPTION OF DATA.	3
II. 14-17 NOVEMBER 1988 SYNOPTIC ANALYSIS	4
A. OVERVIEW.	4
B. LEE CYCLOGENESIS STAGE.	4
C. RAPID DEEPENING STAGE.	6
D. THE FILLING STAGE.	7
E. SUMMARY.	8
III. 03-05 JANUARY 1989 SYNOPTIC ANALYSIS.	23
A. OVERVIEW.	23
B. PRE-CYCLOGENETIC STAGE.	23
C. EXPLOSIVE DEVELOPMENT STAGE.	24
D. THE FILLING STAGE.	25
E. SUMMARY.	26
IV. COMPARISON OF DYNAMICAL FORCING.	42
A. UPPER-LEVEL PROCESSES.	42
B. SURFACE LOW LEVEL FORCING.	43
C. STATIC STABILITY.	46
D. SUMMARY.	47
V. CONCLUSIONS.	60
LIST OF REFERENCES	62
INITIAL DISTRIBUTION LIST	64

LIST OF FIGURES

Fig. 1. Time Series of Land Cyclone Central Pressure.	9
Fig. 2. 1200 UTC 14 November 1988 Sea Level Analysis.	10
Fig. 3. 1200 UTC 14 November 1988 300 mb Analysis.	11
Fig. 4. 0000 UTC 15 November 1988 Sea Level Analysis.	12
Fig. 5. 1200 UTC 15 November 1988 Sea Level Analysis.	13
Fig. 6. 1200 UTC 15 November 1988 300 mb Analysis.	14
Fig. 7. 1200 UTC 15 November 1988 Vertical Cross Section.	15
Fig. 8. 1801 UTC 15 November 1988 GOES IR Imagery.	16
Fig. 9. 0000 UTC 16 November 1988 1000 mb Analysis.	17
Fig. 10. 0000 UTC 16 November 1988 300 mb Analysis.	18
Fig. 11. 0000 UTC 16 November 1988 Vertical Cross Section.	19
Fig. 12. 0501 UTC 16 November 1988 GOES IR Imagery.	20
Fig. 13. 1200 UTC 16 November 1988 Sea Level Analysis.	21
Fig. 14. 1200 UTC 16 November 1988 300 mb Analysis.	22
Fig. 15. Time Series of Ocean Cyclone Central Pressure.	28
Fig. 16. 1200 UTC 03 January 1989 Sea Level Analysis.	29
Fig. 17. 1201 UTC 03 January 1989 GOES IR Imagery.	30
Fig. 18. 1200 UTC 03 January 1989 300 mb Analysis.	31
Fig. 19. 0000 UTC 04 January 1989 Sea Level Analysis.	32
Fig. 20. 0001 UTC 04 January 1989 GOES IR Imagery.	33
Fig. 21. 0000 UTC 04 January 1989 300 mb Analysis.	34
Fig. 22. 0000 UTC 04 January 1989 Vertical Cross Section.	35
Fig. 23. 0600 UTC 04 January 1989 Sea Level Analysis.	36
Fig. 24. 1200 UTC 04 January 1989 Sea Level Analysis.	37
Fig. 25. 1201 UTC 04 January 1989 GOES IR Imagery.	38
Fig. 26. 1200 UTC 04 January 1989 300 mb Analysis.	39
Fig. 27. 0000 UTC 05 January 1989 Sea Level Analysis.	40
Fig. 28. 0000 UTC 05 January 1989 300 mb Analysis.	41
Fig. 29. 0000 UTC 16 November 1988 300 mb Divergence	49
Fig. 30. 1200 UTC 04 January 1989 300 mb Divergence	50
Fig. 31. 1800 UTC 03 January 1989 1000 mb θ Local Change	51

Fig. 32. 0000 UTC 04 January 1989 Temperature Advection Profile	52
Fig. 33. 0600 UTC 04 January 1989 1000 mb θ Local Change	53
Fig. 34. 1200 UTC 04 January 1989 Temperature Advection Profile	54
Fig. 35. 1800 UTC 15 November 1988 1000 mb θ Local Change	55
Fig. 36. 1200 UTC 15 November 1988 Static Stability	56
Fig. 37. 1200 UTC 16 November 1988 Static Stability	57
Fig. 38. 0000 UTC 04 January 1989 Static Stability	58
Fig. 39. 0000 UTC 05 January 1989 Static Stability	59

I. INTRODUCTION.

A. BACKGROUND.

Explosive cyclogenesis is a phenomenon that continues to be examined by many investigators. Sanders and Gyakum (1980) defined explosive cyclone development as a deepening of the cyclone central pressure by one mb per hour for 24 hours. Recently, numerous observational studies of land and maritime rapid cyclogenesis have been conducted. However, there is very little documented work comparing the rapid development of a land cyclone with that of an oceanic storm. Some key mechanisms that need to be examined in a land vs. oceanic case are: the development and magnitude of upper-level forcing, jet streak interactions, low-level heat and moisture fluxes in the boundary layer, static stability magnitude and maintenance, and thermal advection structure and differences. This study will compare these aspects listed above to determine the similarities and differences in the rapid development of a continental and maritime explosive cyclone.

The climatology of rapidly deepening cyclones was initially prepared by Sanders and Gyakum (1980) who concluded that explosive cyclones were predominately maritime events. Roebber (1984) updated the climatology and observed that rapidly deepening cyclones appeared to be a combination of baroclinic processes and some other mechanism(s).

Kocin and Uccellini (1985) conducted extensive analysis of eighteen severe U.S. East Coast cyclones that produced large amounts of snowfall. Some of these cyclones were of continental origin. Kocin and Uccellini observed the significant impact jet streaks and jet streak positioning have on rapid cyclogenesis and comment on the intensification of surface lows under the divergent region of an upper-level jet streak. They found that when the left side exit divergent region of a jet streak in the trough (entrance jet) and the right side entrance divergent region of a jet streak in the ridge (exit jet) are co-located, maximum upper-level divergence is generated over the surface low. This positioning will be referred to as optimum positioning of the jet streaks in later discussion. While the jet streak in the upstream trough seems to be characteristic of many cyclones, the jet streak in the downstream ridge resulted from confluence between the ridge and a trough to its north over eastern Canada. A strong surface anti-cyclone to the northeast of the developing cyclone was characteristic of this upper-level confluent pattern.

Analysis of some recent cyclones illustrate some differences between coastal and oceanic cyclones. Uccellini et al (1984) conducted a detailed study of the Presidents' Day storm of February 1979. They noted the presence of two distinct jet streaks in the upstream trough and downstream ridge of this coastal cyclone. Conversely, Reed and Albright (1986) studied a rapidly intensifying cyclone over the eastern North Pacific Ocean. This cyclone developed without a downstream jet streak.

The low-level forcing and diabatic processes in explosive cyclones has been studied and results vary widely. Bosart and Lin (1984) examined the diabatic heating and formation of low level jets for the Presidents' Day storm. Uccellini et al (1987) conducted numerical model studies of the same storm and concluded that both diabatic processes and jet streak interactions contributed in the development of the coastal cyclone. Nuss and Kamikawa (1990) studied two cyclones along the coast of Japan and concluded that the surface heat and moisture fluxes in an explosive and non-explosive cyclone vary significantly. From these studies, there appears to be a link between boundary layer processes, diabatic effects and jet streak interactions, at least in the maritime environment. It remains to be demonstrated that these interactions make the maritime cyclone significantly different than the continental storm.

Reed and Albright (1986) comment on the presence of low static stability in the baroclinic environment as being one of the causes of their rapid cyclogenesis in a maritime case. Kocin and Uccellini (1985) also note some periods of low static stability during intense coastal cyclones. Further study is needed to show that low static stability is a common feature of all maritime and continental rapidly developing storms.

The two storms chosen for study in this thesis occurred during winter 1988-1989. The land development case originated during 14-17 November 1988. A small surface cyclone, originating over western Oregon propagated to the southeast without much development. When the cyclone was in the vicinity of the Texas panhandle, deepening commenced and the cyclone moved to the northeast. Rapid development soon followed and this cyclone achieved rapid development criteria (1 mb hr) after 1200 UTC 16 November 1988. This cyclone eventually reached 974 mb before it started to fill.

The ocean case started as a small surface disturbance along the Carolina-Virginia coast which began explosive development on 04 January 1989. In the space of 24 hours, this storm deepened from 996 mb to 936 mb, easily meeting all criteria for rapid development. This maritime cyclone developed typically for a strong rapid development as described by Sanders (1986). The storm propagated to the northeast very rapidly and was accompanied by strong 500 mb vorticity maximum. As the storm reached maturity,

a tight, circular cloud pattern could be observed around the cyclone center. This cloud configuration is very similar to the intense cyclone analyzed by Reed and Albright (1986) in the eastern North Pacific Ocean.

It appears that there has not been recent comparative studies of land and oceanic cyclones using the same diagnostic approach. The aims of this paper are twofold: first, to document the development of an explosive land and oceanic cyclone; second, utilizing the same diagnostic approach, evaluate and compare the forcing mechanisms that caused these two storms to rapidly develop. Synoptic analysis and development of the individual storms are provided in sections 2 and 3. A comparison and analysis of the upper- and lower-level forcings and static stability of the two cyclones is given in section 4. Figures are provided at the end of each section and concluding remarks can be found in section 5.

B. DESCRIPTION OF DATA.

For the continental case, the National Meteorological Center's Nested Grid Model (NGM) analysis fields and the Spectral Grid Model (SGM) analysis fields obtained in the Interactive Digital Environmental Analysis Lab (IDEA lab) at the Naval Postgraduate School were used for the appropriate time periods of the cyclone. The GEMPAK software available in the IDEA Lab was used to analyze various storm parameters such as vorticity advection and upper-level divergence. GOES satellite IR and visual imagery were also available.

The maritime case was analyzed using the National Meteorological Center's Spectral Grid Model analysis obtained in the IDEA Lab for the Intense Observation Period 4 (IOP 4) of the ERICA experiment conducted during the winter of 1988-89. The IDEA Lab was also used for analysis of the various fields along with GOES satellite data. Surface analysis by Sanders (1989) was used for diagnosis of the surface patterns during the maritime development.

The NMC Spectral Model has less resolution than the Nested Grid Model. The comparison of the NGM and SGM fields in these two cases was done with the realization that some error might be introduced in the comparison due to potential lack of detail in the Spectral model fields. To minimize this problem, SGM fields for the land case were used in the comparison of specific diagnostic fields where possible. Significant deviations between the SGM and NGM grids for the land cyclone have been identified and are discussed. Other potential errors, due to the different grids, when comparing the two cyclones are also noted.

II. 14-17 NOVEMBER 1988 SYNOPTIC ANALYSIS.

A. OVERVIEW.

The intense cyclone that developed over the central U.S. between 1200 UTC 14 November 1988 and 1200 UTC 17 November 1988 provides an example of fairly rapid land cyclogenesis. As shown in Fig. 1, the cyclone deepened from 992 mb to 974 mb between 1800 UTC 15 November 1988 and 1800 UTC 16 November 1988 yielding an average deepening rate of 18mb/24 h, which is very close to the criterion for explosive cyclogenesis given by Sanders and Gyakum (1980). The time series of central pressure (Fig. 1) suggests three distinct periods in the lifecycle of this cyclone. The first period from 1200 UTC 14 November 1988 to 1200 UTC 15 November 1988 is characterized by lee cyclogenesis east of the Rocky Mountains and the progression of a high amplitude upper-level trough across the western U.S. and is called the lee cyclogenesis stage. The second period from 1200 UTC 15 November 1988 to 1800 UTC 16 November 1988 is the rapid deepening stage where the lee cyclone over the Texas Panhandle develops and propagates northeast to Minnesota. This period is called the rapid deepening stage. The final period, from 1800 UTC 16 November 1988 to 1200 UTC 17 November 1988, is the filling stage where the central pressure increases while the cyclone continues to propagate eastward and is called the filling stage.

B. LEE CYCLOGENESIS STAGE.

The synoptic analysis for 1200 UTC 14 November 1988 depicts the incipient stage of lee cyclogenesis east of the Rocky Mountains. The NGM sea-level pressure analysis (Fig. 2) shows two 1002 mb low centers. The northern low center over Idaho is the parent low that has propagated inland from the coast. This low center is positioned under the left exit region of a 300 mb jet streak (Fig. 3) which provides upper-level support for this primary surface feature. The southern low over Utah is a new development along the cold front associated with the Idaho cyclone. Little upper-level support is found with this second low. There is no 500 mb vorticity center in the vicinity of the southern cyclone and entrance and exit divergence regions of the 300 mb jet are not positioned near the low. A significant feature in the surface analysis is the pressure trough that extends from the primary low down through Wyoming to the Texas Panhandle. Palmen and Newton (1969) describe the formation of a pressure trough in the lee of the Rocky Mountains in response to adiabatic heating due to down slope flow as the air moves over

the mountains and onto the plain. Warm advection to the east of the trough and continued down slope flow widen the pressure trough. Orographically-caused pressure falls will be further enhanced when positive vorticity advection (from the propagation of the upper-level trough eastward over the mountains) contributes to cyclonic development. In this cyclone, the pressure trough appears to develop as described by Palmen and Newton and forms the warm frontal boundary associated with the parent low. Strong warm advection at 850 mb (not shown) east of the trough supports this interpretation of lee cyclogenesis. The lee trough is primarily a low-level feature and occurs under anticyclonically curved flow and convergence aloft (Fig. 3).

During the next 12 hours, the sea-level pressure pattern evolved significantly. A single low formed over northern Colorado while the lee trough intensified to the south and a weaker inverted trough formed to the north (Fig. 4). A strong warm front has developed and propagated north from Kansas to the Kansas-Nebraska border. A 20 °F temperature difference is found across the warm front. There appears to be very little upper-level forcing associated with the surface cyclone. The 500 mb positive vorticity advection is located in Arizona, southwest of the surface cyclone. Again, there is also very little upper-level divergence in the vicinity of the low.

Analysis of surface reports during the next 12 hours shows that the cyclone propagates from northern Colorado into east-central Colorado and to the Texas-Oklahoma Panhandle by 1200 UTC 15 November 1988 (Fig. 5). This southward propagation of the surface cyclone is consistent with the eastward advance of the strong upper-level forcing over Arizona. With this southward movement, the inverted trough and warm frontal boundary have merged. A strong low-level warm front is found across Kansas, Nebraska, Iowa, Illinois and Michigan.

There is now favorable phase relationship between the 993 mb surface cyclone and the 300 mb trough. The deep trough previously over Arizona has moved eastward rapidly and is directly upstream in relation to the surface cyclone. The vorticity advection from the upper-level trough (not shown) is now placed directly over the surface low giving a favorable westward tilt between the 300 mb trough and the surface cyclone. This indicates that this system is baroclinically unstable and should develop. The strong 300 mb vorticity advection results from a 96 kt jet (Fig. 6) which is located in the base of the upper-level trough. Additionally, a strong short wave at 500 mb has propagated down over southwestern Canada.

Ahead of the warm front, an 84 kt jet has developed and is downstream from the strong 300 mb short wave previously mentioned. The IR imagery shows a cirrus cloud

edge along the axis of the northern jet streak. This streak is providing strong shear vorticity for the upper short wave in southern Canada. The right side entrance divergence region of the northern jet is located over the South Dakota - Iowa - Minnesota border area. The strong upper wave over Canada and the deep trough behind the cyclone create a region of confluence over South Dakota. This area will later become very important to the rapid development of the cyclone.

Fig. 7 presents a vertical cross section ahead of the surface cyclone. (Stations can be located on Fig. 6). Evidence of the downstream jet is located along the RAP station profile between the 300-200 mb levels. The upstream jet is above DDC with a 120 kt maximum wind indicated. This cross section confirms the presence of both an up-and downstream jet streak in the vicinity of the cyclone. The warm front is also clearly depicted between LBF and DDC.

C. RAPID DEEPENING STAGE.

At 1500 UTC 15 November 1988, the cyclone had a pressure of 992 mb and had commenced movement to the northeast, apparently tracking along the warm front. The 1801 UTC 15 November 1988 IR imagery (Fig. 8) gives a good depiction of the cyclone's cloud patterns over the Kansas-Oklahoma border. The inner circulation of the cyclone appears to be relatively small and well-organized, with strong convection along the distinct cold front that extends southward through central Oklahoma. The warm front is associated with the edge of the deeper clouds through Minnesota and Wisconsin. By 0000 UTC 16 November 1988, the cyclone central pressure dropped to 988 mb and is located in southern Iowa. The cold front extends through Arkansas and Texas (Fig. 9) while a warm front curves through Michigan and across the Great Lakes. From surface reports, a strong cold surge (20 kt surface wind from the north) is evident over the Dakotas and Nebraska.

The upper-level forcing has also intensified during the past twelve hours. The 500 mb analysis (not shown) shows further amplification of the upper wave. The short wave trough in Canada has also deepened. Strong vorticity values and PVA continue to suggest upper-level divergence over the cyclone. At 300 mb (Fig. 10), the left side exit divergence region of the entrance jet and the right side entrance divergence region of the exit jet are aligned over Iowa suggesting an intense, localized region of upper-level divergence directly over the surface cyclone. Fig. 11 is a vertical cross section (stations found on Fig. 10) ahead of the surface cyclone. The exit jet between HON and OVN is centered at between 300-200 mb with an 95 kt maximum. The entrance jet is at TOP

with 120 kt maximum around 400 mb. This cross section shows a dual entrance-exit jet configuration quite similar to those described by Kocin and Uccellini (1985). Additionally, the velocity of the exit jet has increased presumably as a result of a warm front temperature gradient increase which is not well reflected in the sparse surface data.

During the next few hours, the cyclone tracks along the warm front. At 0300 UTC 16 November 1988, the central pressure drops to 987 mb. The 0501 UTC 16 November 1988 IR image shows the cyclone near the Minnesota-Iowa border (Fig. 12). The cyclone has grown significantly in size since 1801 UTC 15 November 1988. The cloud band along the cold front has doubled in length with heavy convection along its entirety. The cloud shield associated with this cyclone now extends from southern Canada to Texas. By 1200 UTC 16 November 1988, the cyclone central pressure has now lowered to 979 mb and is located over Lake Superior (Fig. 13.). The warm front continues to extend northward over the Ontario region. The cold front curves through Michigan, Indiana, Illinois, Missouri and across into Texas.

Extremely strong upper-level forcing coincided with the deepening cyclone. The 500 mb trough and short wave have combined into a deep wave behind the cyclone with the upper wave amplitude continuing to be large. The exit jet has intensified to 108 kt (not shown) while the entrance side jet streak has a velocity of 120 kt (Fig. 14.). The divergent regions of both jets continue to be aligned and generally over the surface cyclone.

In the next few hours, the cyclone continues to deepen and move north-northeast. At 1500 UTC 16 November 1988, the central pressure reaches 976 mb. The 1601 UTC 16 November 1988 IR image clearly shows the cyclone, which appears to be occluded. However, the strong upper-level vorticity and divergence continue to deepen the cyclone. The lowest central storm pressure, 974 mb, was attained at 1800 UTC 16 November 1988.

D. THE FILLING STAGE.

The cyclone fills during the next 24 hours, reaching 979 mb by 0000 UTC 17 November 1988 while located north of Lake Superior. The 500 mb low is almost directly over the surface low, indicating occlusion. Loss of baroclinic tilt is an indicator of cyclone dissipation. At 300 mb, the exit jet has propagated over the ridge and is no longer in optimal position to increase divergence over the cyclone. The entrance jet remains strong, but the left side exit divergence region is not favorably located over the low. The 0001 UTC 17 November 1988 IR imagery shows the cyclone continuing to occlude. The cold front has moved to the east and is no longer associated with the

cyclone. The warm front and some associated jet streak cirrus are visible over the Hudson Bay region. Strong PVA is still present aloft but it is located well ahead of the surface cyclone. Also, cold thermal advection at the cyclone center is serving to raise sea-level pressure.

E. SUMMARY.

In summary, this cyclone shows three distinct stages of development. The first stage involved lee cyclogenesis in association with a weak low that had propagated over southern Wyoming. The main feature of this parent cyclone was a lee pressure trough and warm front extending to the southeast. The presence of low-level warm southerly advection east of the cyclone and the proximity of the pressure trough to the Rocky Mountains confirms that this lee cyclone was principally a low-level feature. Also, there was an inverted trough north of the warm front. There was little upper-level forcing associated with this cyclone during this stage as lee cyclogenesis processes dominated.

The rapid development occurred in the second stage of the cyclone. The initial lee cyclone propagated southeast over the Texas Panhandle while a strong 300 and 500 mb trough moved eastward upstream of the cyclone position. A 96 kt jet streak at 300 mb was embedded in the trough and suggests there is upper-level divergence over the surface low. The low propagated to the northeast and began development. Meanwhile, a strong exit jet developed in response to the thermal gradient found along the cyclone warm front and the eastward advance of a shortwave over southern Canada. Interaction of the entrance and exit jet streaks suggests large upper-level divergence values to deepen the cyclone. The cyclone reached its lowest pressure while under strong upper-level forcing.

The final stage occurred when the upper-level forcing of the cyclone ended. The cyclone began to fill as it lost baroclinic energy and upper-level support. The jet streaks propagated out of position and no longer enhanced divergence. Additionally, the positive vorticity advection was not in best position to produce divergence over the surface low. The cyclone slowly filled and propagated to the east.

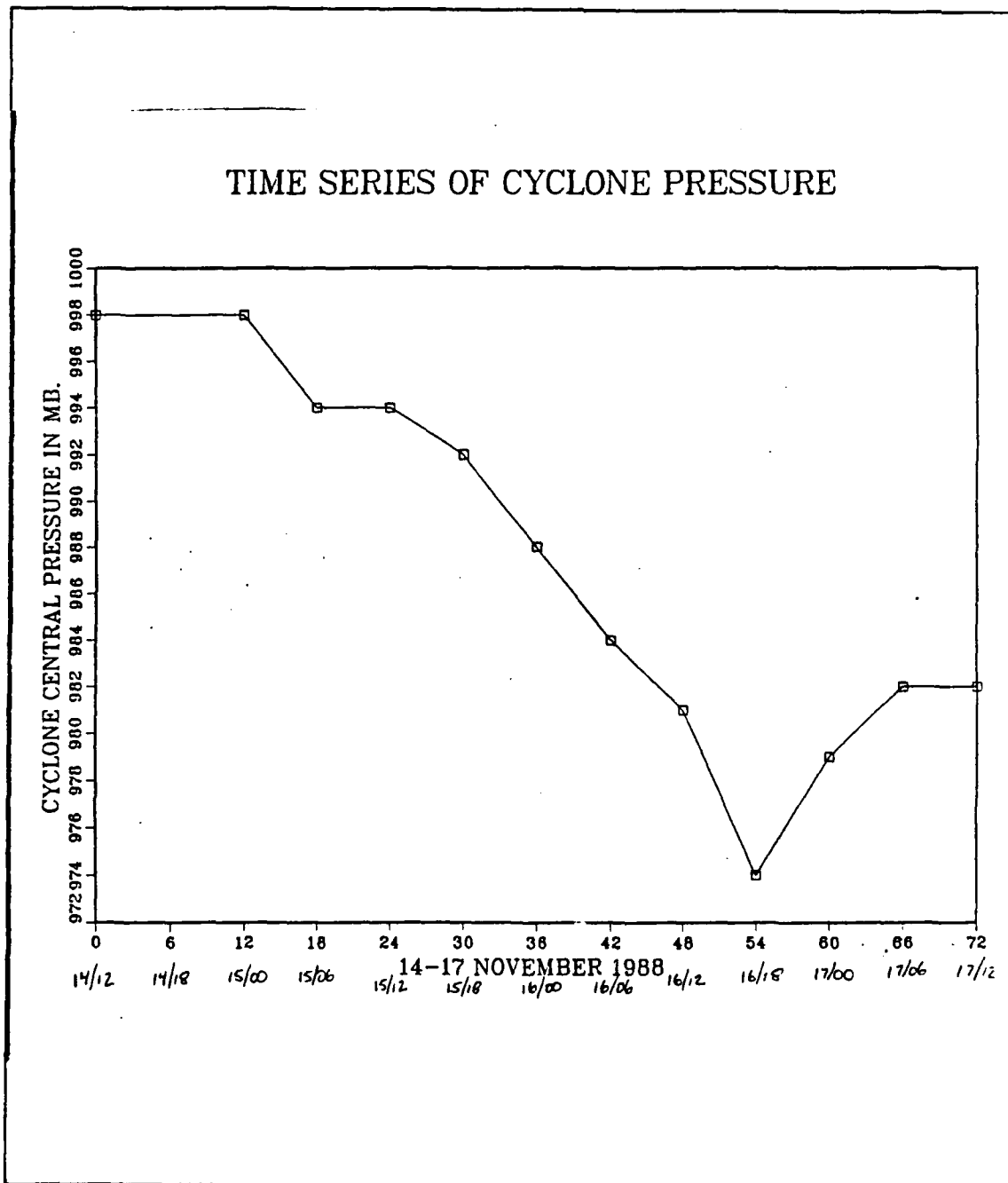


Fig. 1. Time Series of Land Cyclone Central Pressure.: Time 0 represents 1200 UTC 14 November 1988. Time interval in 6 hour periods.

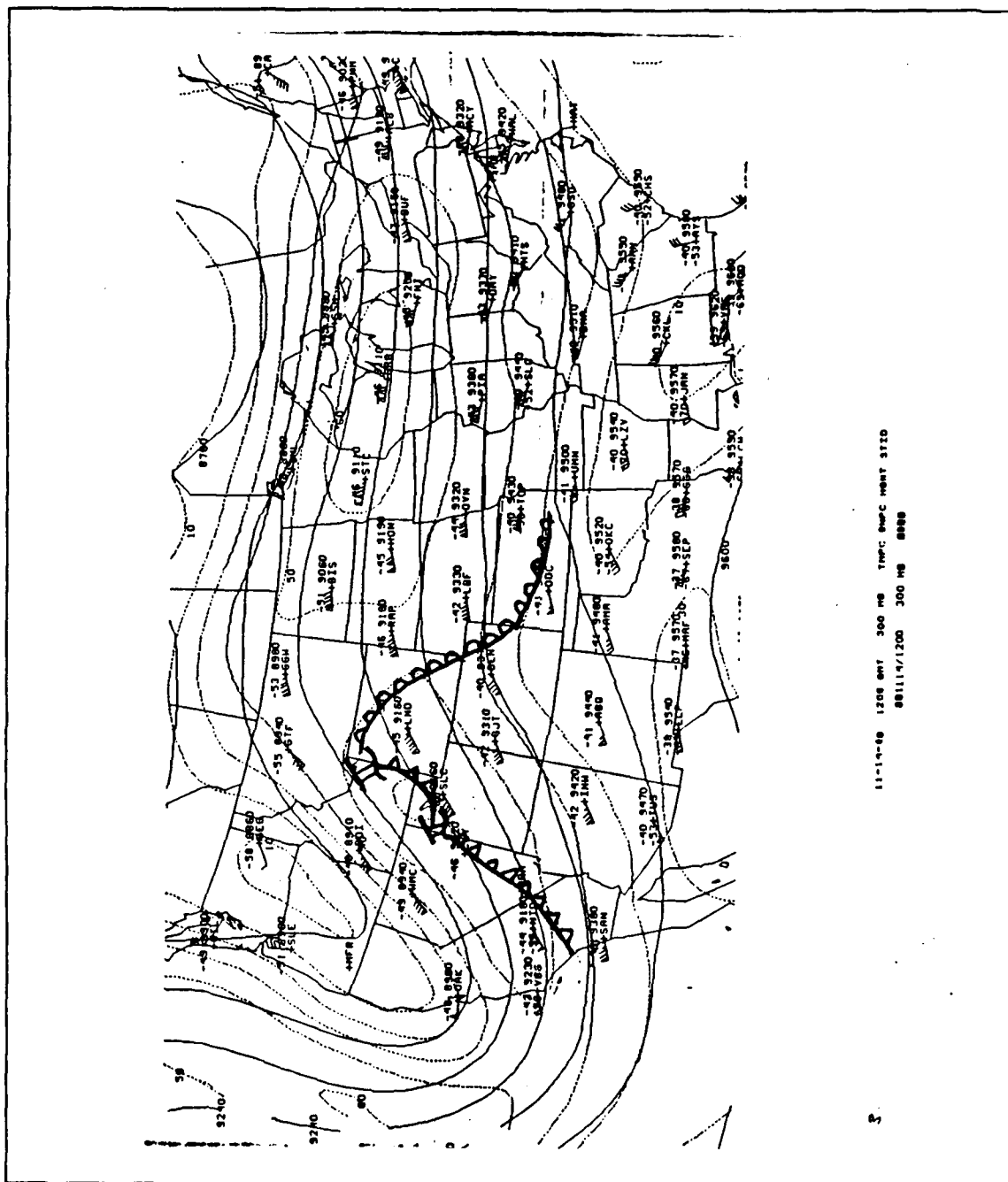


Fig. 3. 1200 UTC 14 November 1988 300 mb Analysis.: Solid lines are geopotential height (m) and dashed lines are isotachs (m/s). Plotted winds are in knots.

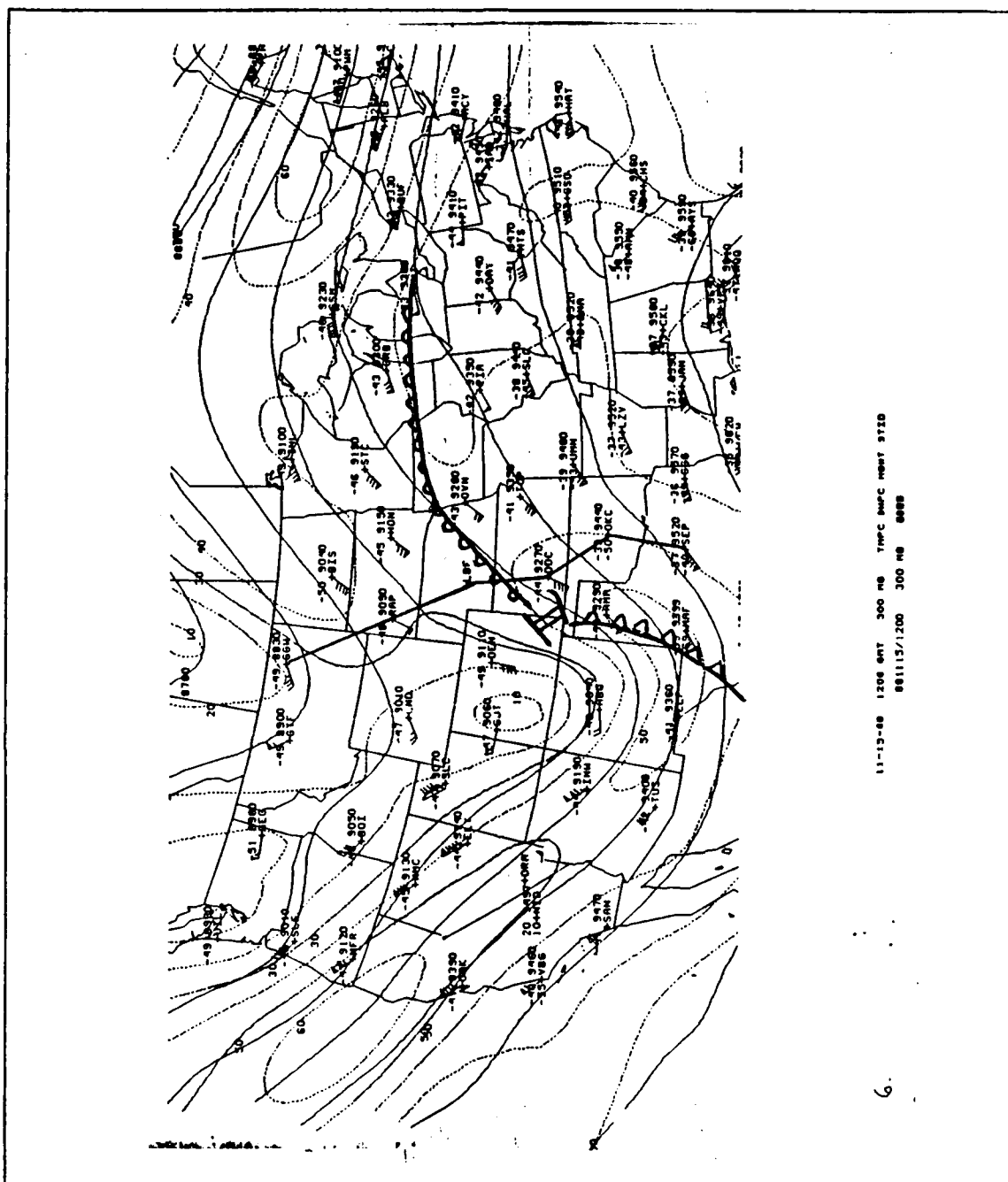


Fig. 6. 1200 UTC 15 November 1988 300 mb Analysis.: Solid lines are geopotential height (m) and dashed lines are isotachs (m/s). Plotted winds are in knots.

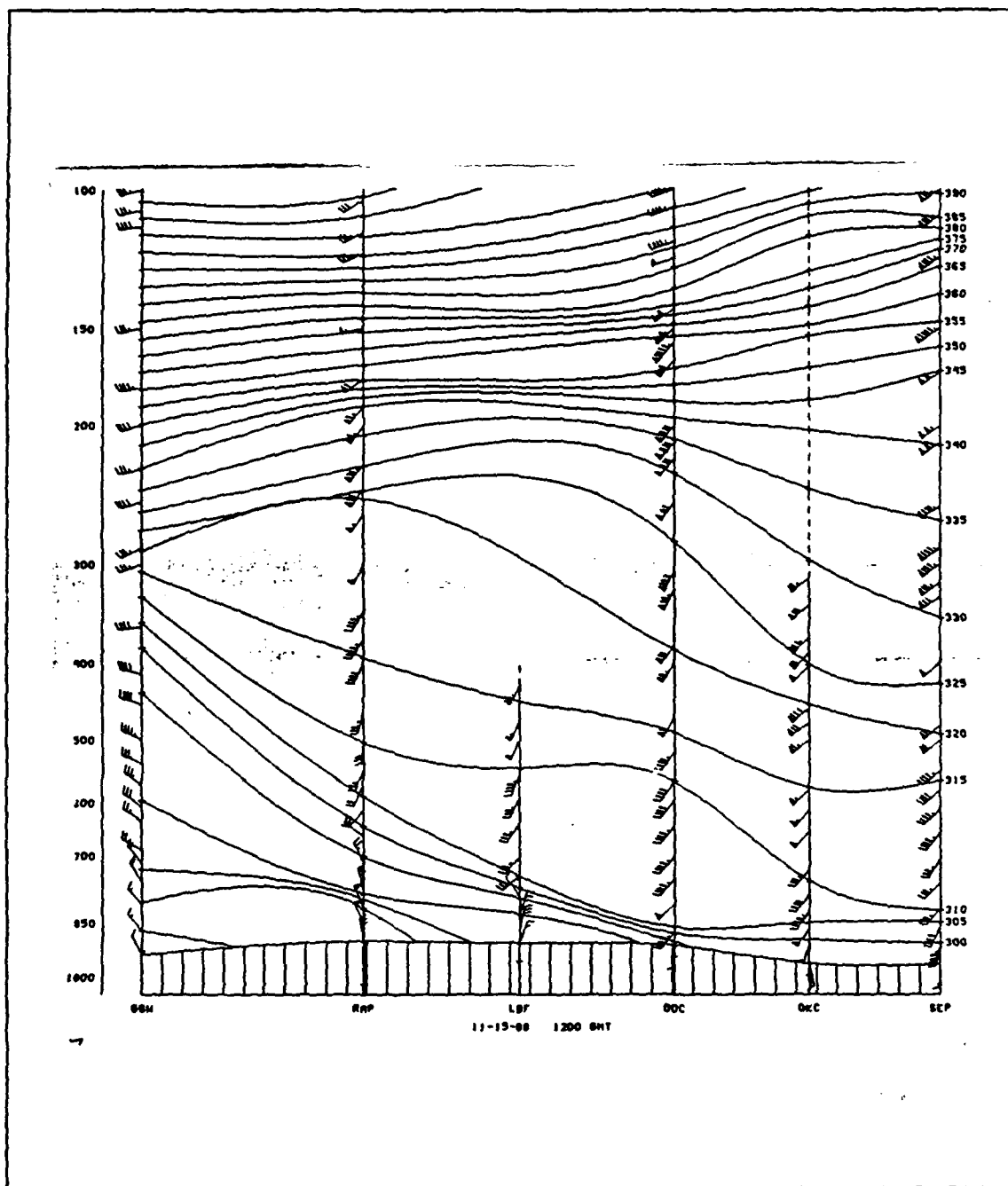


Fig. 7. 1200 UTC 15 November 1988 Vertical Cross Section.: Solid lines are θ values. Plotted winds are in knots.

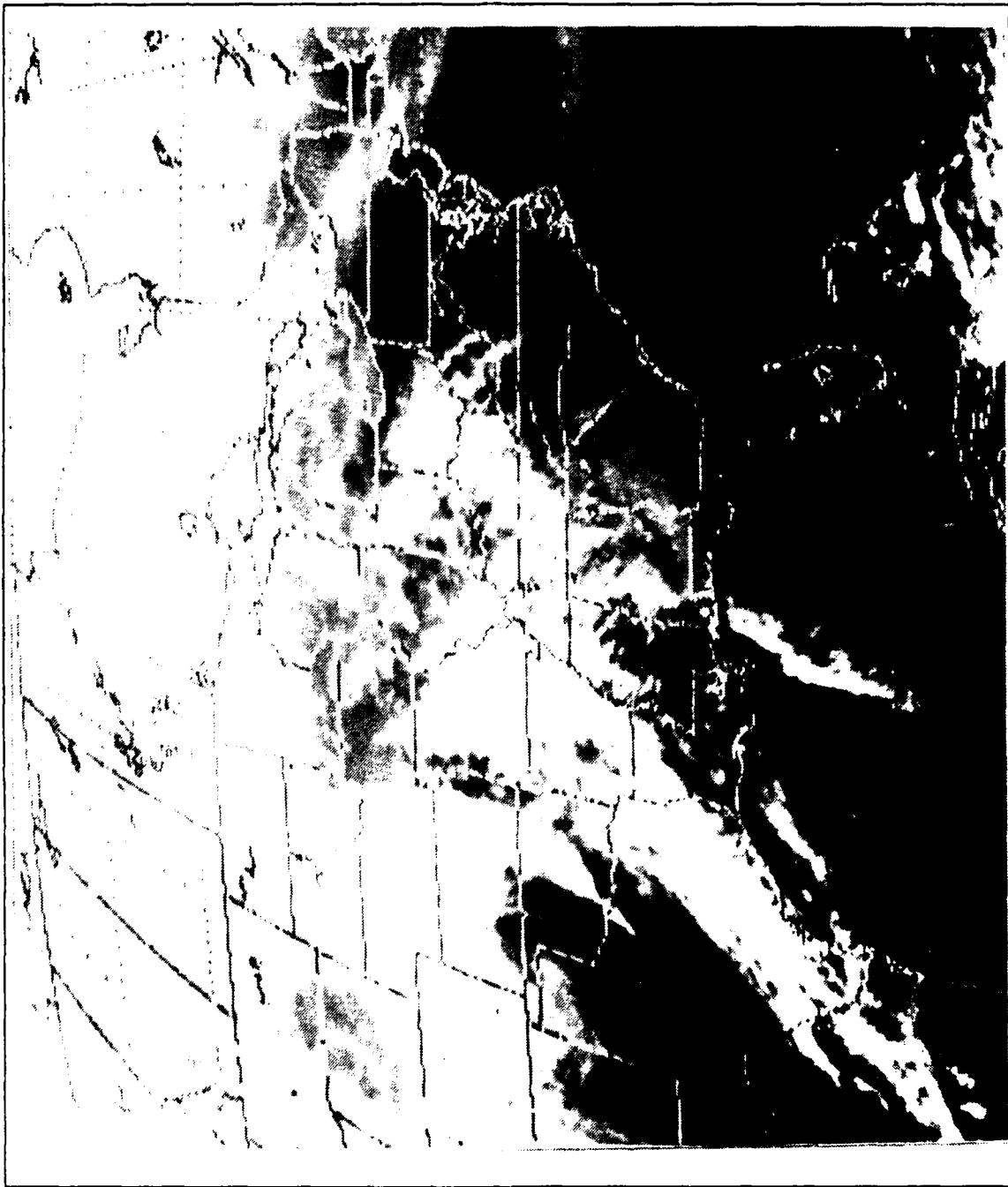


Fig. 8. 1801 UTC 15 November 1988 GOES IR Imagery.

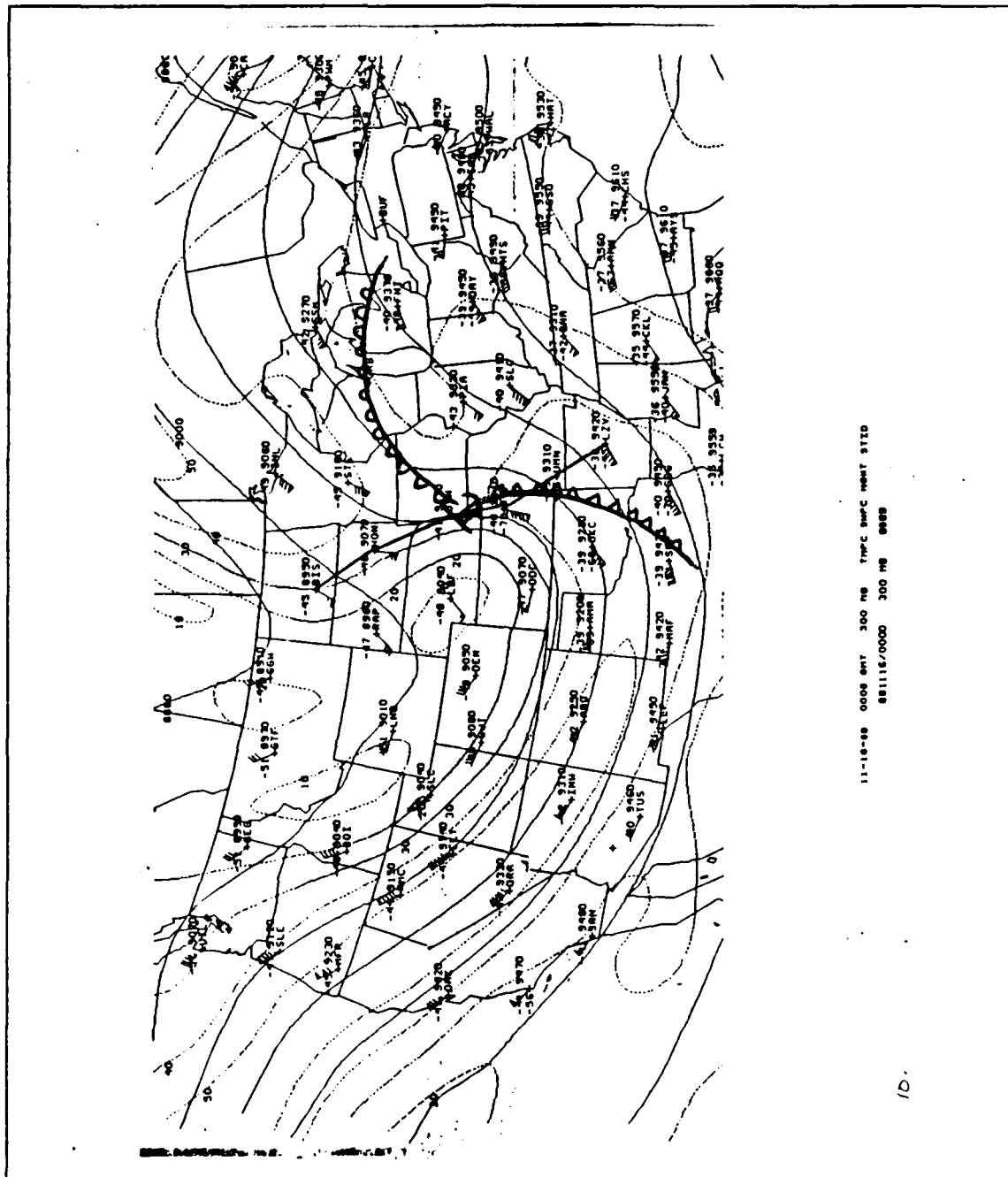


Fig. 10. 0000 UTC 16 November 1988 300 mb Analysis.: Solid lines are geopotential height (m) and dashed lines are isotachs (m/s). Plotted winds are in knots.

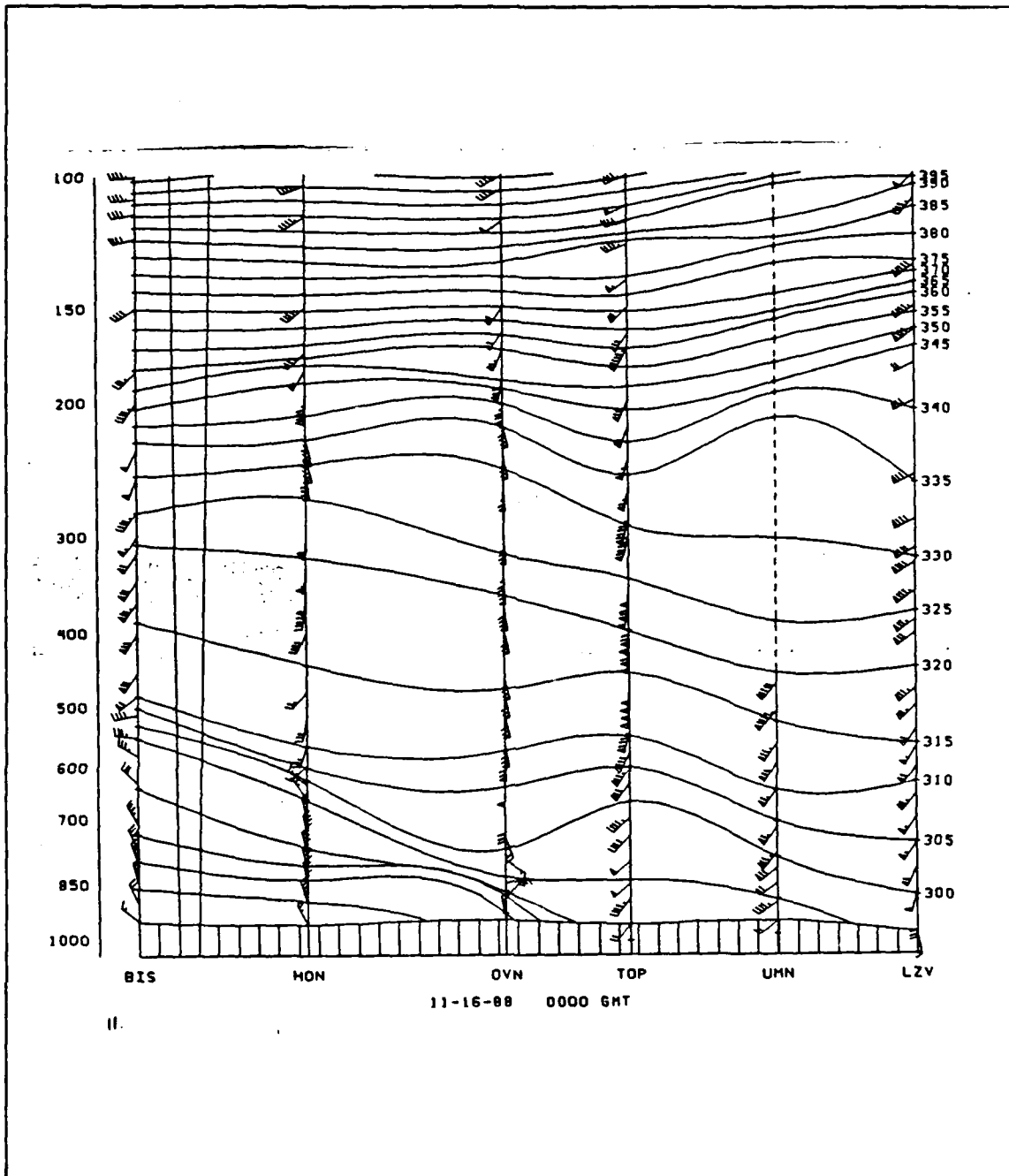


Fig. 11. 0000 UTC 16 November 1988 Vertical Cross Section.: Solid lines are θ values. Plotted winds are in knots.



Fig. 12. 0501 UTC 16 November 1988 GOES IR Imagery.

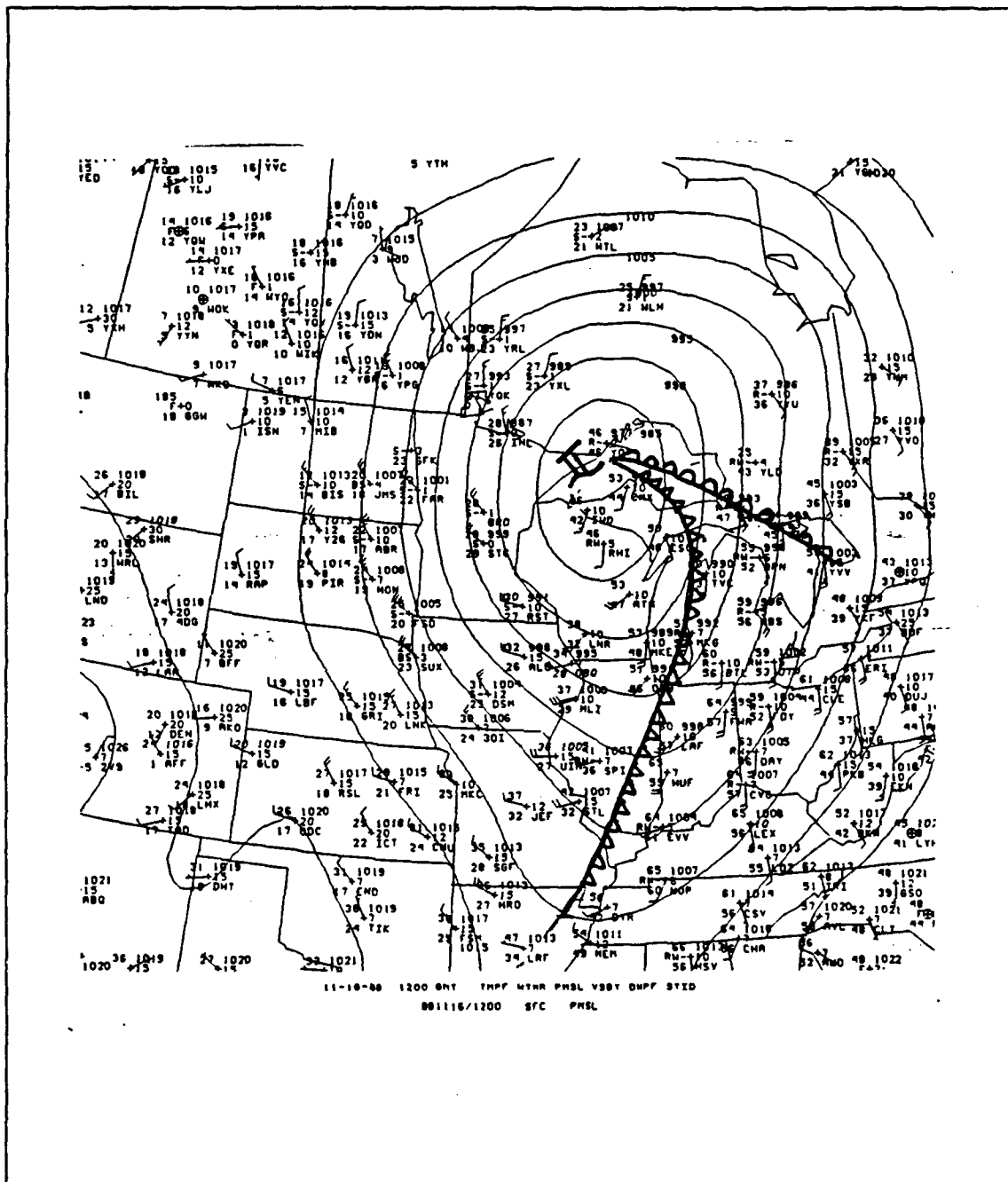


Fig. 13. 1200 UTC 16 November 1988 Sea Level Analysis.: Solid lines are in 5 mb increments.

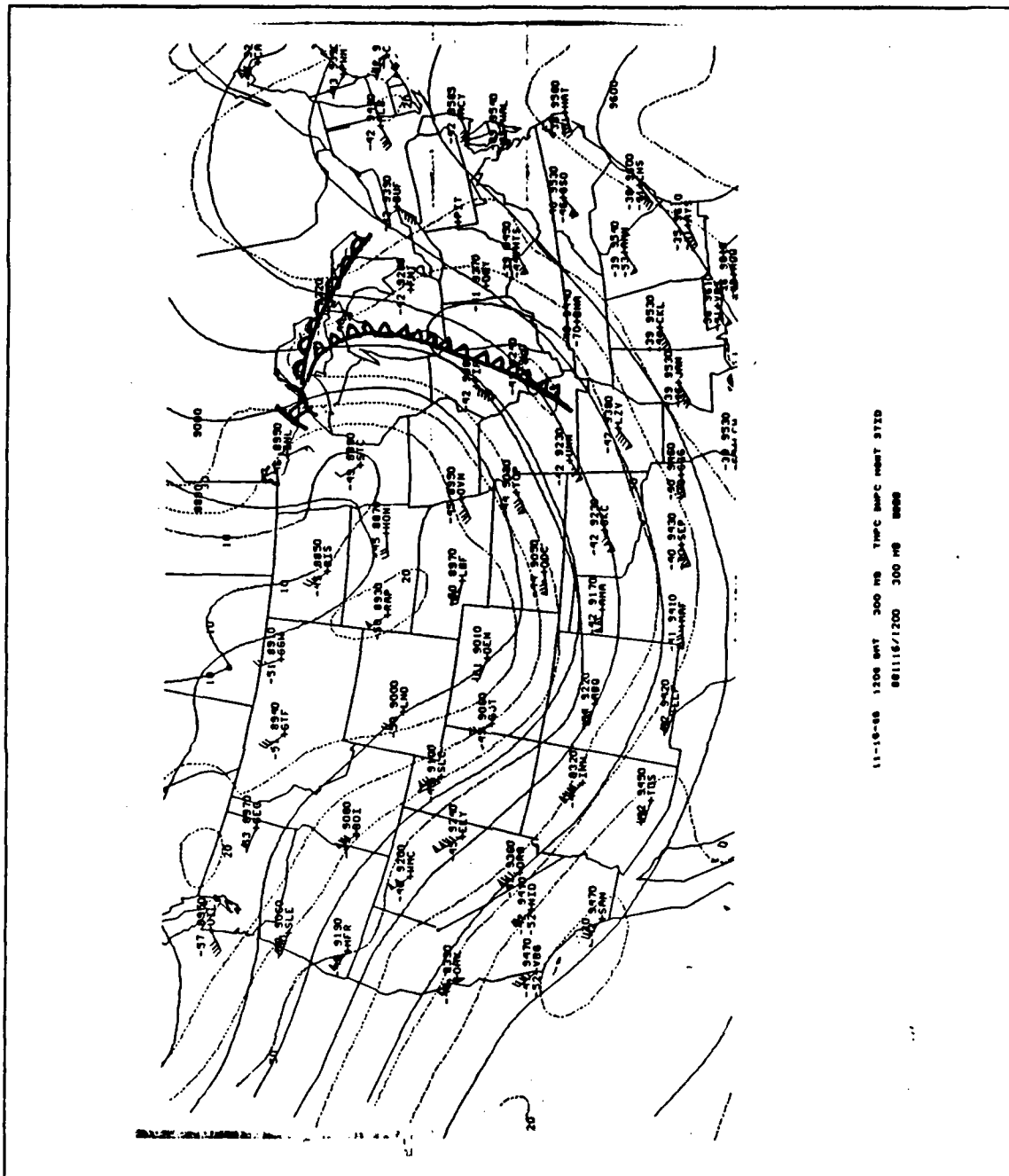


Fig. 14. 1200 UTC 16 November 1988 300 mb Analysis.: Solid lines are geopotential height (m) and dashed lines are isotachs (m/s). Plotted winds are in knots.

III. 03-05 JANUARY 1989 SYNOPTIC ANALYSIS.

A. OVERVIEW.

An explosive cyclone developed off of the U.S. East Coast between 0000 UTC 04 January 1989 and 0000 UTC 05 January 1989. This cyclone rapidly deepened from 996 mb to 936 mb in 24 hours. This corresponds to a development rate of 2.5 mb/hr, easily satisfying the criterion for explosive cyclogenesis! The central pressure trace of rapid cyclone development is given in Fig. 15. There appears to be three stages in the life of this cyclone. The first stage from 1200 UTC 03 January 1989 to 0000 UTC 04 January 1989 is the pre-cyclogenetic stage (not shown in Fig. 15) with a strong upper-level jet streak positioned over the Carolina-Virginia coast and a strong vorticity center over the Great Lakes region. The second phase of this cyclone, from 0000 UTC 04 January 1989 to 0000 UTC 05 January 1989, is called the explosive development stage and commences when the upper-level jet streak mentioned above produces a small 996 mb surface low by 0000 UTC 04 January 1989. Rapid deepening commenced when the strong vorticity center previously mentioned propagated immediately upstream of the surface low. Intense deepening occurred as the cyclone propagated to the northeast. A dual entry-exit jet streak configuration formed to enhance upper-level divergence and allowed for further development. The final stage occurred when the cyclone moved from the relatively low static stability environment and commenced to fill after 0000 UTC 05 January 1989 and is referred to as the filling stage. The following sections will examine these stages in detail.

B. PRE-CYCLOGENETIC STAGE.

The 1200 UTC 03 January 1989 synoptic analysis characterizes the pre-cyclogenetic environment of this very intense cyclone. The surface analysis (Fig. 16) shows cold northwesterly flow dominating the western North Atlantic Ocean in the wake of a fairly strong cyclone now situated to the southeast of Nova Scotia. The cold air has not propagated very far to the south over the coastal waters off of the middle East Coast as shown by the surface isotherms in Fig. 16. Of particular note is the deep band of clouds that extends from the Ohio valley well out into the western North Atlantic Ocean. (Fig. 17). This band indicates substantial moisture and vertical motion throughout the troposphere and has anticyclonic curvature over Kentucky and Virginia. The NMC Spectral 300 mb analysis (Fig. 18) shows a strong 144 kt jet streak over Kentucky and

Virginia that extends out into the western North Atlantic. When comparing the IR imagery and the 300 mb isotach analysis, it appears that the analysis did not extend the core of the jet streak far enough into the western Atlantic. The strong convection extending from the Virginia Coast, as depicted in Fig. 17, provides evidence of the presence of a jet streak over the water. The jet streak would provide strong cyclonic shear vorticity advection and upper-level divergence which would enhance the convective activity. The strong upper-level vorticity center and 500 mb trough (not shown) located over Lake Michigan subsequently influences cyclone development.

During the next 12 hours, warm surface advection (not shown) from the south can be found along southeastern coast of the U.S., replacing the northwesterly flow by 1800 UTC 03 January 1989. A strong band of convection continues to extend from the western Carolinas into the North Atlantic ocean.

C. EXPLOSIVE DEVELOPMENT STAGE.

By 0000 UTC 04 January 1989, a new 996 mb sea-level low has developed over the mouth of the Chesapeake Bay (Fig. 19.). This low develops very rapidly during the next 24 hours to become a 936 mb low at 0000 UTC 05 January 1989. Warm surface advection along the southern East Coast has increased dramatically, with a 45 kt low-level jet at the surface being reported off the North Carolina coast. The 0001 UTC 04 January 1989 IR image (Fig. 20) still shows the deep cloud band extending out from the coast of the Carolinas associated with the incipient cyclone.

At the upper levels, a very strong 500 mb trough has developed from the trough previously over Michigan, in the area to the west of the weak cyclone. This strong trough suggests strong vorticity advection located directly west of the weak surface cyclone. The strong vorticity is a result of an intense 160 kt 300 mb jet streak (Fig. 21). The left side exit divergence region of this upstream jet is located directly over the weak surface cyclone. A vertical cross section along selected east coast stations (Fig. 22) shows the 155 kt jet is visible over GSO (stations listed in Fig. 21). A strong upper-level front is also visible on this cross section. A weak ridge has formed 500 nmi east of the Carolina coast with a portion of the previously mentioned jet streak embedded. The static stability over the water is low (not shown).

By 0300 UTC 04 January 1989, the central pressure of the new cyclone is 983 mb. The 0301 UTC 04 January 1989 IR image (not shown) begins to show the typical comma shaped pattern of a mid-latitude cyclone. At 0600 UTC 04 January 1989 (Fig. 23.), the cyclone central pressure is 976 mb and is located approximately 150 nmi east

of Delaware. The surface temperature gradient across both the warm and cold fronts is small. A large cloud shield is also visible over the cyclone and to the north and east.

By 1200 UTC 04 January 1989, the central pressure has reached 960 mb (Fig. 24). The surface temperature gradient across the cold front of the cyclone remains small. However, there is some significant deformation of the isotherms near the cyclone center. This isotherm deformation is a good indicator of intensification of a strong temperature gradient, which implies that baroclinic energy is available for continued cyclone development. Low level winds of 50 kt from the northwest are being reported behind the cold front while 60 to 70 kt winds from the southwest are reported in the warm sector ahead of the cold front. There appears to be very strong convergence generated by these winds along the cold front. Static stability values were determined by subtracting the 1000 mb θ value from the 500 mb θ and dividing by the vertical change in pressure. The static stability value (not shown) remains very low in the general cyclone vicinity. The 1201 UTC 04 January 1989 IR image (Fig. 25) shows a well developed and intense cyclone. Heavy convection is located along the cold front southeast of the cyclone. Heavy cloudiness along the warm front to the north and east of the cyclone gives a good indication of the strong warm advection taking place. A strong cold surge from the northwest behind cyclone is present as evidenced by the 20 to 30 kt northwest wind and freezing temperatures being reported along the U.S. east coast.

At 500 mb, a deep trough has amplified from the previous time. Strong vorticity and intense PVA are available to provide upper-level forcing. The 300 mb analysis (Fig. 26) now reflects this forcing and shows a dual jet streak configuration. The upstream entrance side jet streak has a speed of 144 kt. The left side exit divergence region of this jet is in the vicinity of the cyclone and is enhancing the upper-level divergence over the cyclone. The broad area of 100 kt wind downstream from the cyclone suggests the presence of an exit jet streak (Fig. 26). This broad exit jet may also enhance the upper-level divergence over the cyclone. It is possible that a more intense core is embedded inside this large jet structure.

D. THE FILLING STAGE.

At 0000 UTC 05 January 1989, the cyclone central pressure has reached 936 mb (Fig. 27.) and fills from this point on. From the 0001 UTC 05 January 1989 IR image (not shown) the cyclone cloud pattern looks less organized at this time. The center of the cyclone has lost the tight spiral appearance it had eight hours earlier and the cold front has increased in width and is not as sharply defined on the IR image. However, the

cold front structure appears relatively unchanged with strong convergence still reflected by the surface wind reports along the cold front. A very strong warm front gradient has developed to the east of the cyclone. This increase in temperature gradient is also reflected at the upper-levels by an increase in jet streak speed to 116 kt from 100 kt 12 hours earlier.

The 500 mb wave has become more distorted, forming a closed upper-low over the Canadian Maritime provinces. The 500 mb trough is deep with very tight spacing of the pressure surfaces indicative of strong amplification aloft. Strong PVA is still located upstream from the surface cyclone. The 300 mb upstream jet stream has diminished in speed to 128 kt (Fig. 28). This indicates that the temperature gradient has decreased, possibly at the mid-levels. The jet streak has propagated around the 300 mb trough, however, the left side exit divergence region still has positioning to enhance upper-level divergence over the surface cyclone. The right side entrance divergence region of the downstream jet remains in the vicinity of the cyclone to apparently enhance upper-level divergence. This entrance-exit jet streak positioning appears to be very important to explosive cyclogenesis.

Even in the face of strong upper-level forcing, the surface cyclone continues to fill. The static stability around the cyclone has become significantly greater as the cyclone propagates over the cooler waters of the Labrador current. The static stability value at 1200 UTC 05 January 1989 in the cyclone center is approximately two times as great as the 1200 UTC 04 January 1989 value. This loss of low static stability will be explored in the discussion chapter.

E. SUMMARY.

In summary, this cyclone was generated from an area of pre-cyclogenetic upper-level divergence (provided by jet streak positioning) just off the coast of southern Virginia. An area of strong upper-level vorticity was positioned over Michigan. As the upper vorticity propagated over the small surface low, it intensified explosively, producing the second development phase of this cyclone. As the cyclone rapidly propagated to the northeast and over the warm Atlantic waters, upper-level forcing continued to be available in the form of strong PVA. A dual entrance-exit jet streak configuration was apparent during the rapid intensification of this storm. This jet streak positioning was also noted during the intensification of the continental storm, described in the previous chapter. The static stability was very low over the general area of the cyclone development.

In the final stage of this cyclone, the upper-level forcing remained very strong, however the static stability increased dramatically as this cyclone propagated over the cooler waters of the Labrador current. This increase in static stability apparently contributed to the filling of the cyclone.

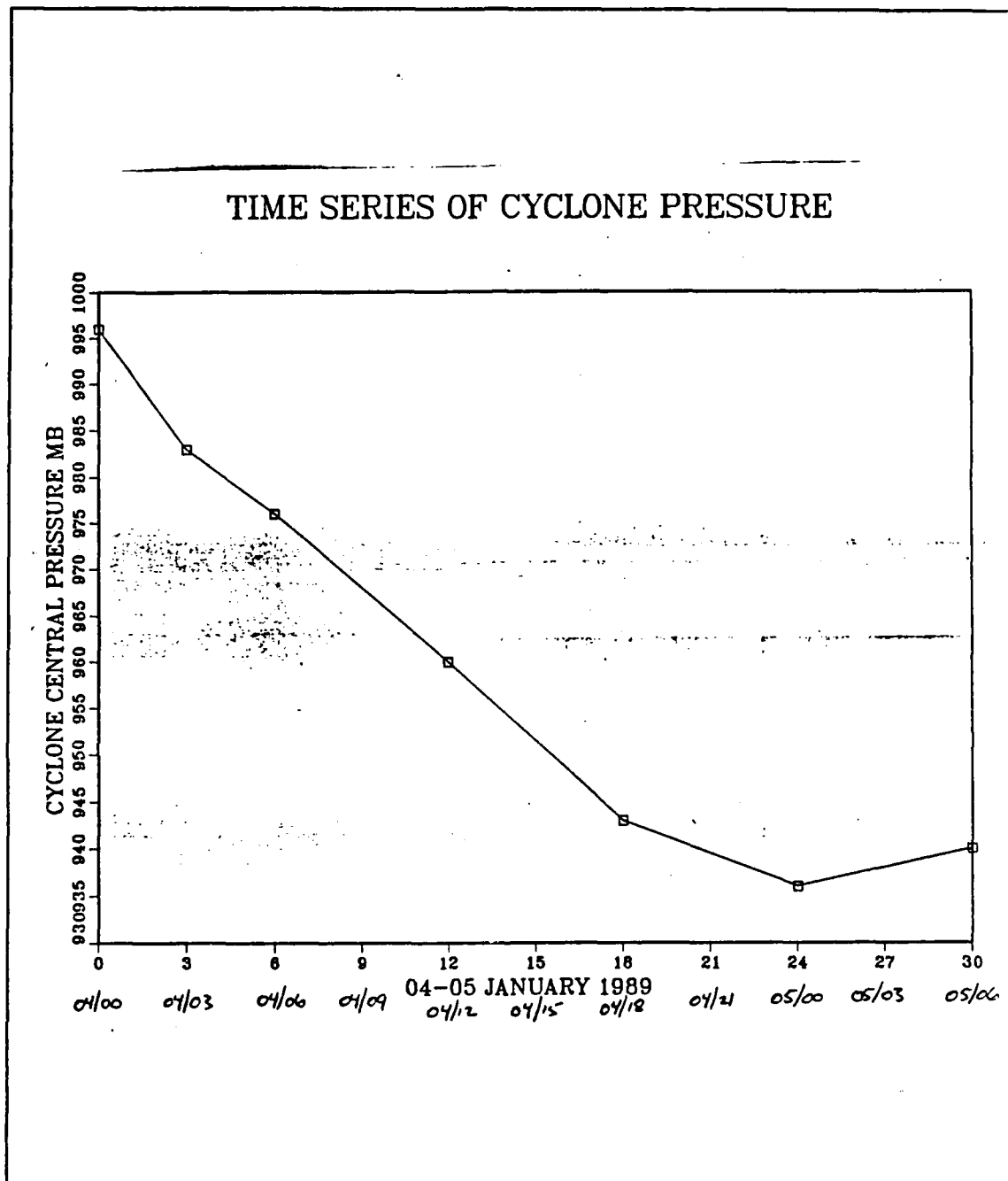


Fig. 15. Time Series of Ocean Cyclone Central Pressure.: Time 0 represents 0000 UTC 04 January 1989. Time interval in 03 hour periods.

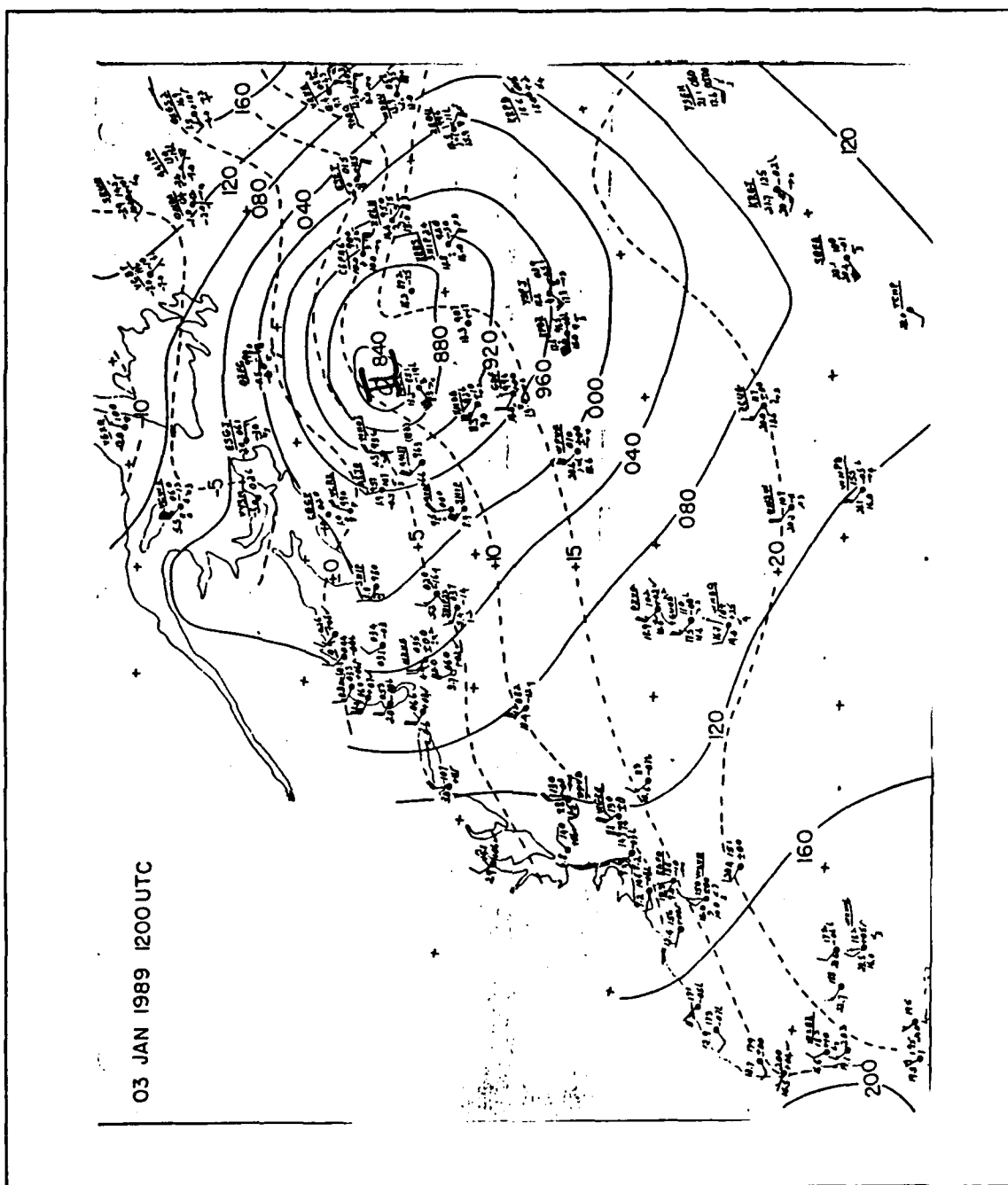


Fig. 16. 1200 UTC 03 January 1989 Sea Level Analysis.: Solid lines are 4 mb intervals. Dashed lines are 05 ° C isotherms.



Fig. 17. 1201 UTC 03 January 1989 GOES IR Imagery.

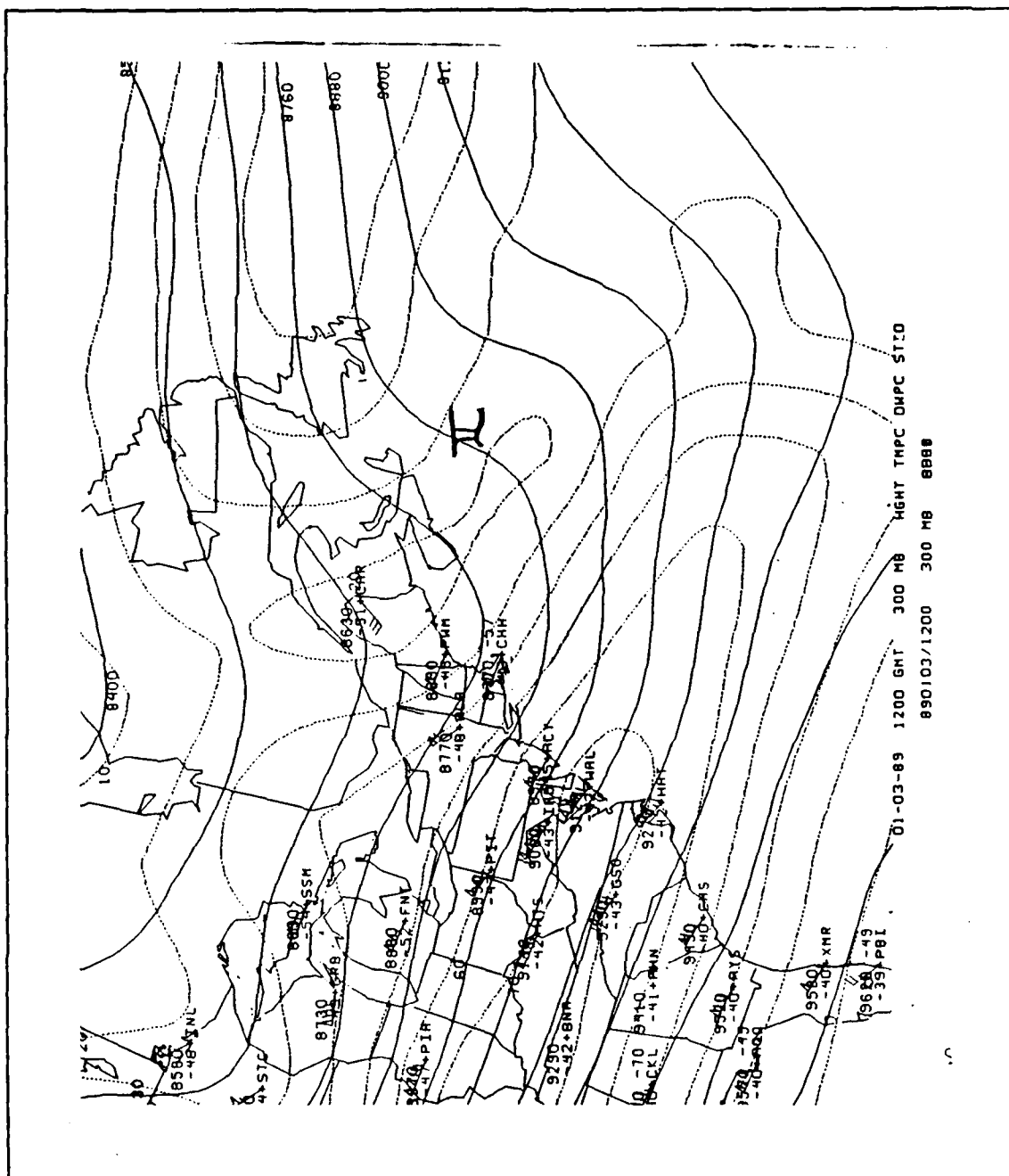


Fig. 18. 1200 UTC 03 January 1989 300 mb Analysis.: Solid lines are geopotential height (m). Dashed lines are isotachs (m/s). Plotted winds are in knots.

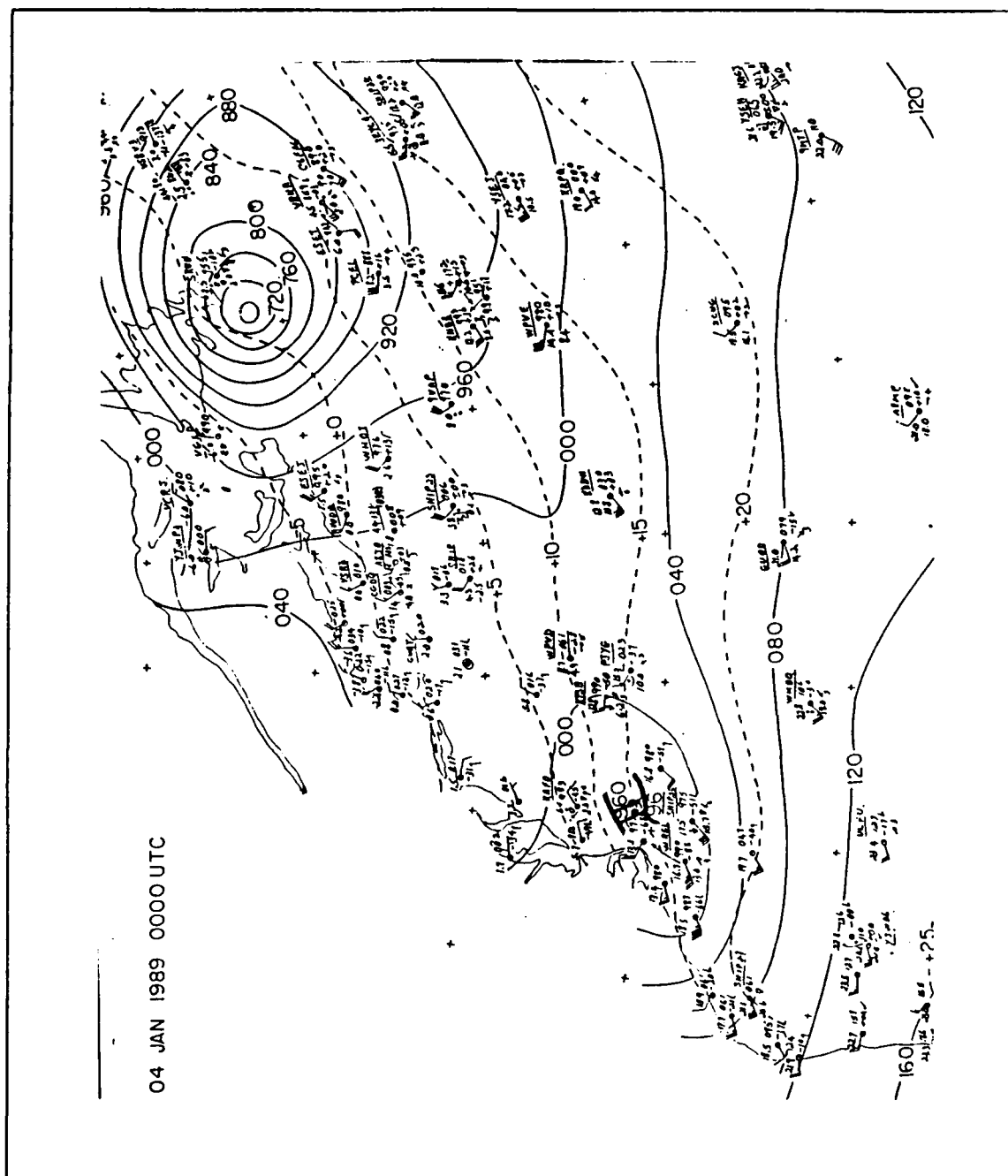


Fig. 19. 0000 UTC 04 January 1989 Sea Level Analysis.: Solid lines are 4 mb intervals. Dashed lines are 05 ° C isotherms.

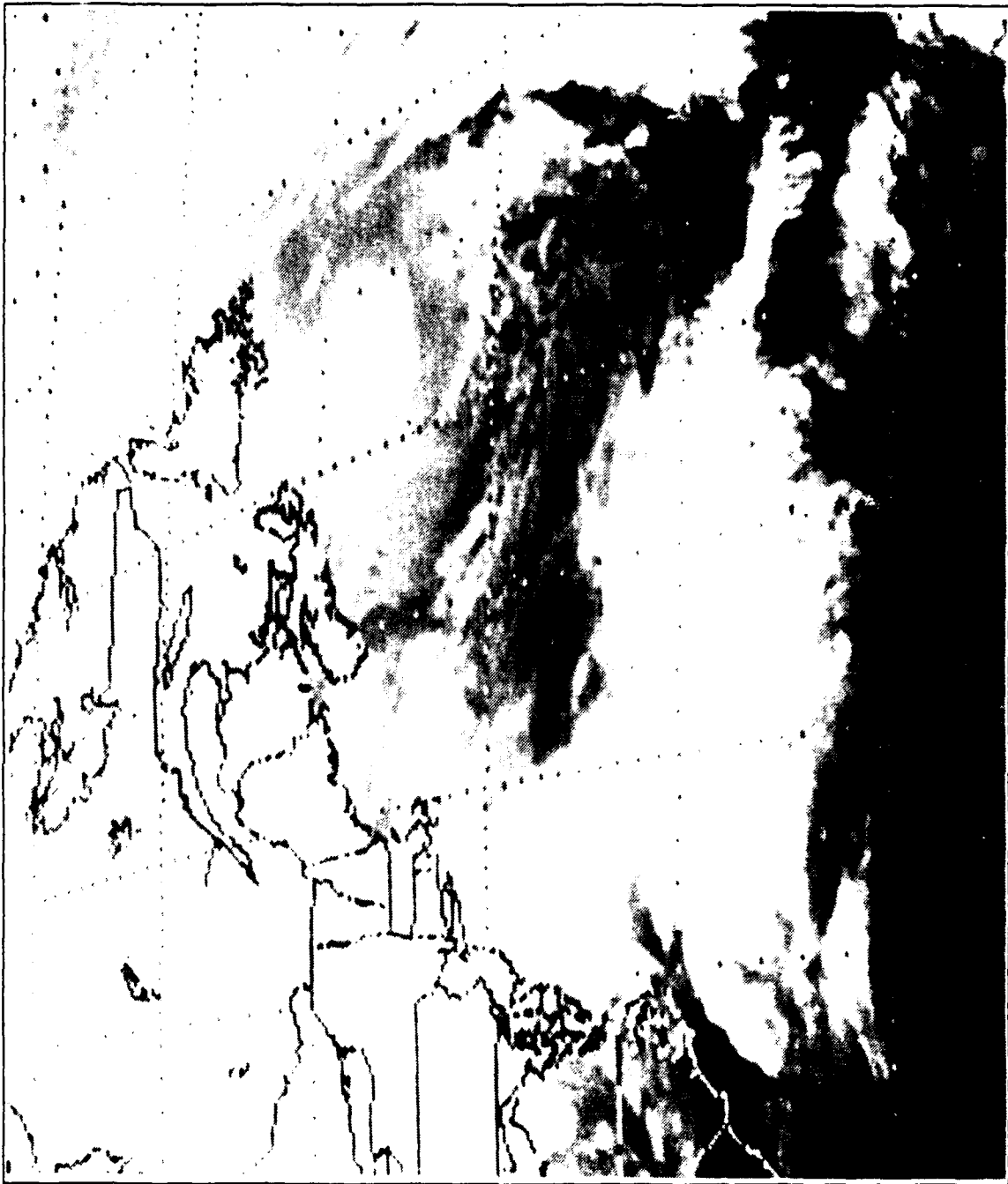


Fig. 20. 0001 UTC 04 January 1989 GOES IR Imagery.

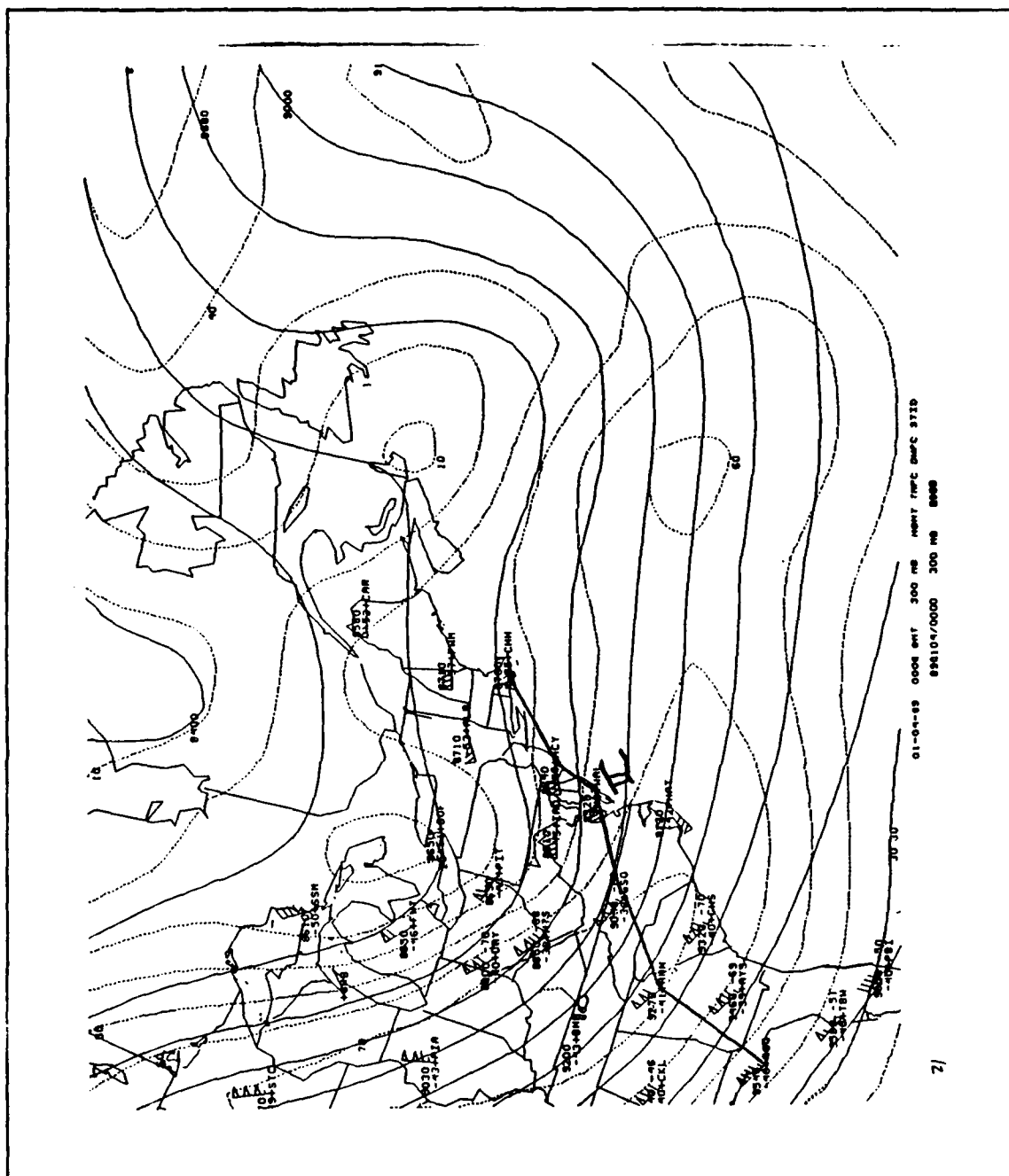


Fig. 21. 0000 UTC 04 January 1989 300 mb Analysis.: Solid lines are geopotential height (m). Dashed lines are isotachs (m/s). Plotted winds are in knots.

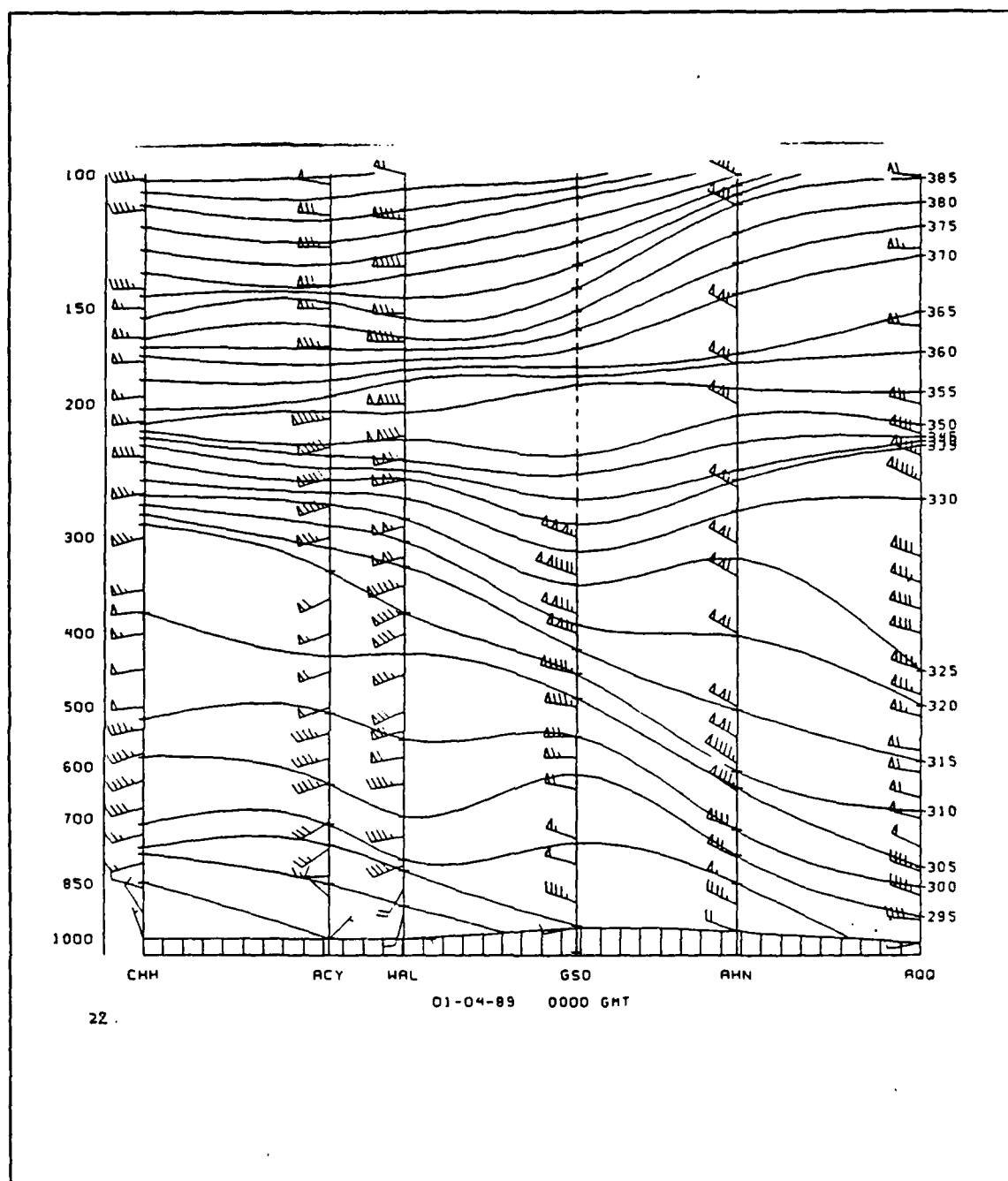


Fig. 22. 0000 UTC 04 January 1989 Vertical Cross Section.: Solid lines are θ values. Plotted winds are in knots.

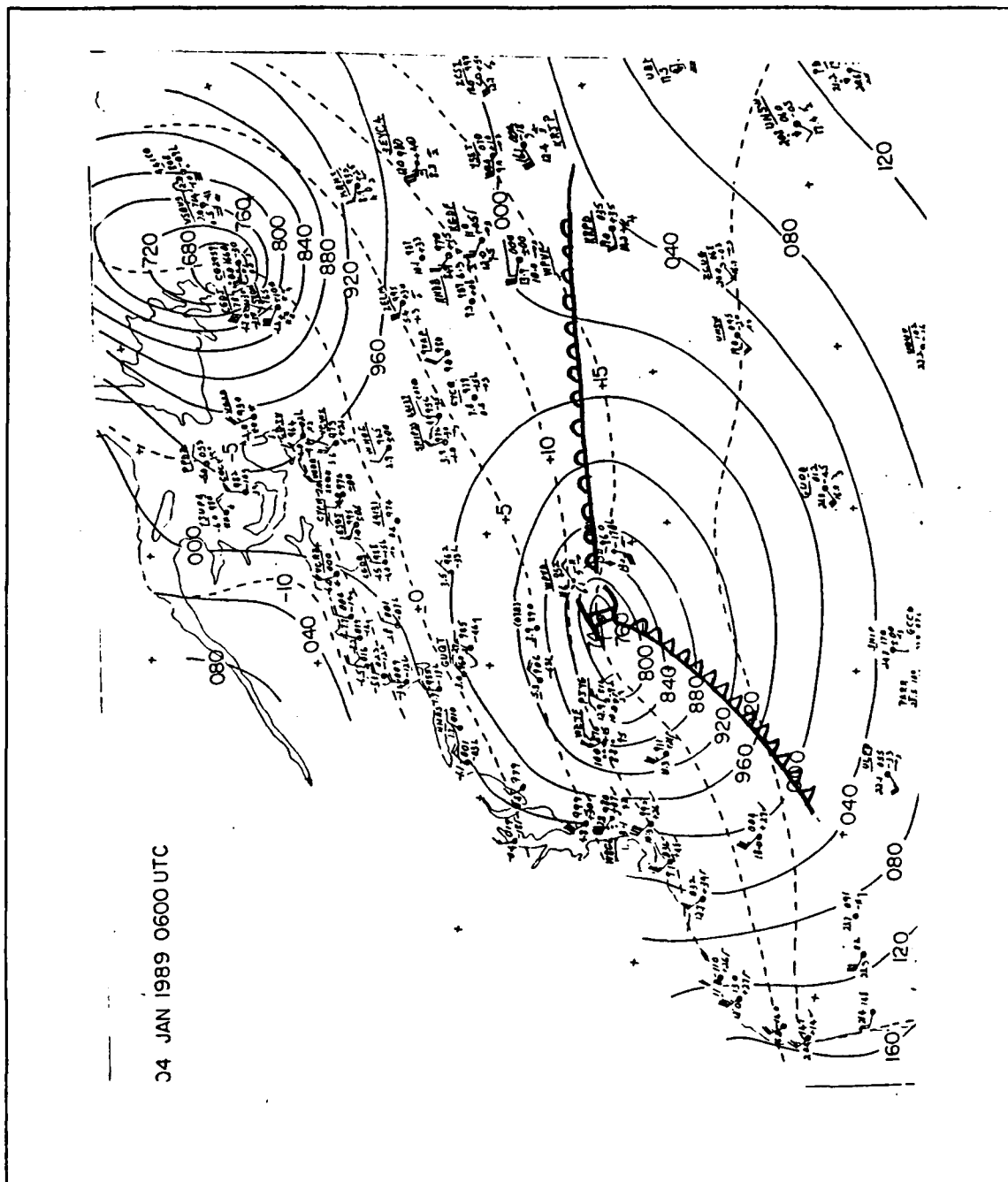


Fig. 23. 0600 UTC 04 January 1989 Sea Level Analysis.: Solid lines are 4 mb intervals. Dashed lines are 0.5 °C isotherms.

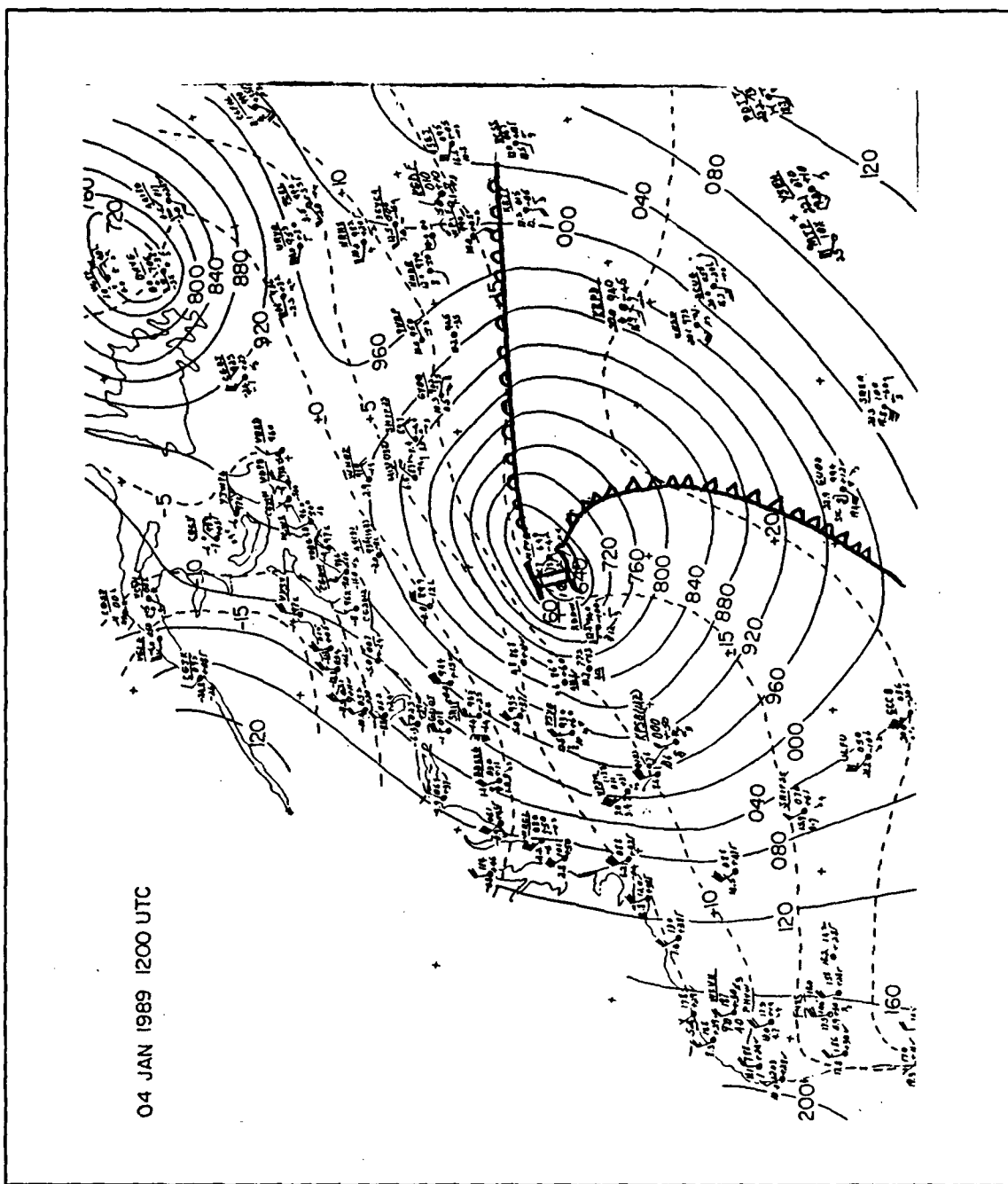


Fig. 24. 1200 UTC 04 January 1989 Sea Level Analysis.: Solid lines are 4 mb intervals. Dashed lines are 0.5 °C isotherms.

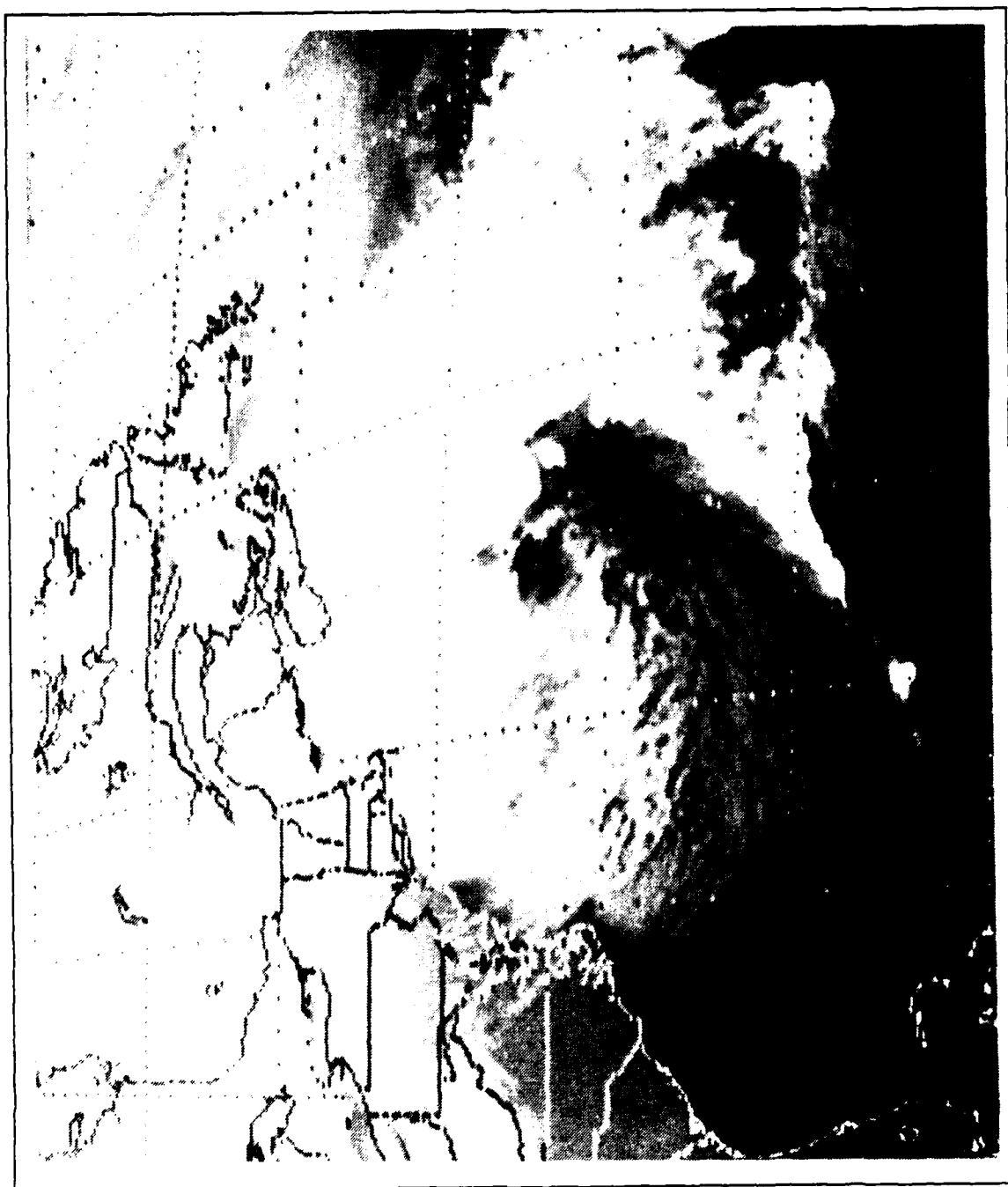


Fig. 25. 1201 UTC 04 January 1989 GOES IR Imagery.

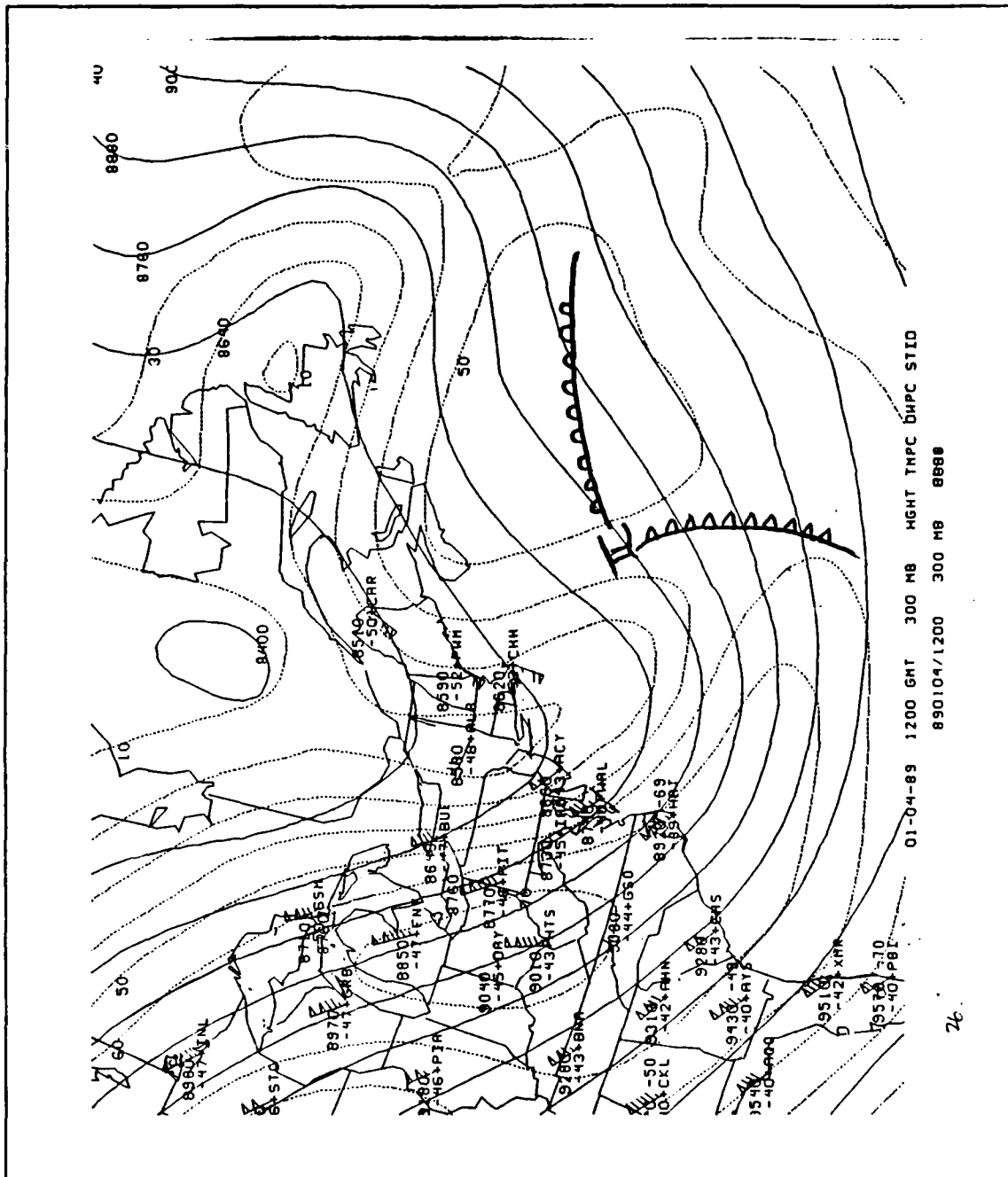


Fig. 26. 1200 UTC 04 January 1989 300 mb Analysis.: Solid lines are geopotential height (m). Dashed lines are isotachs (m/s). Plotted winds are in knots.

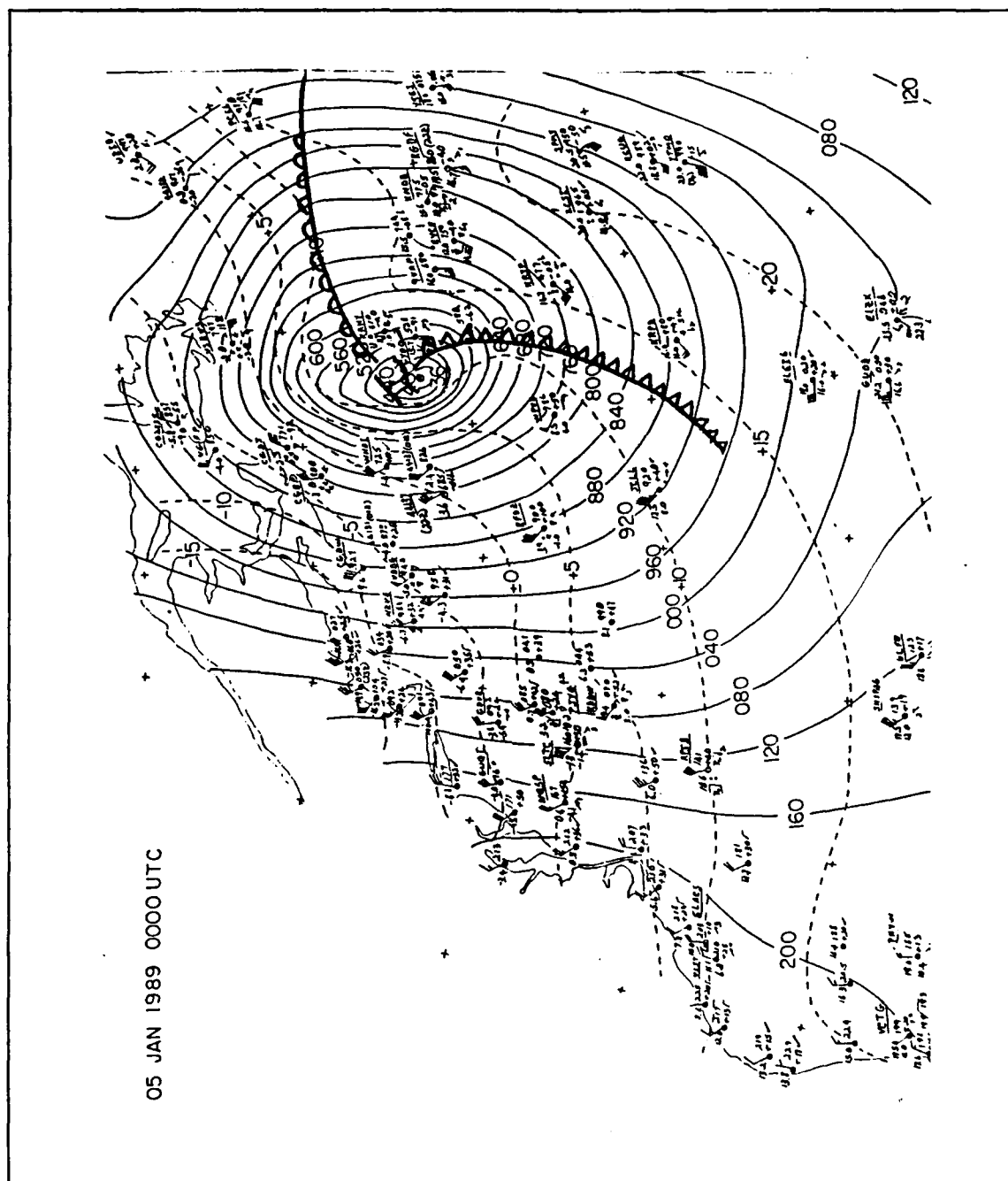


Fig. 27. 0000 UTC 05 January 1989 Sea Level Analysis.: Solid lines are 4 mb intervals. Dashed lines are 0.5 ° C isotherms.

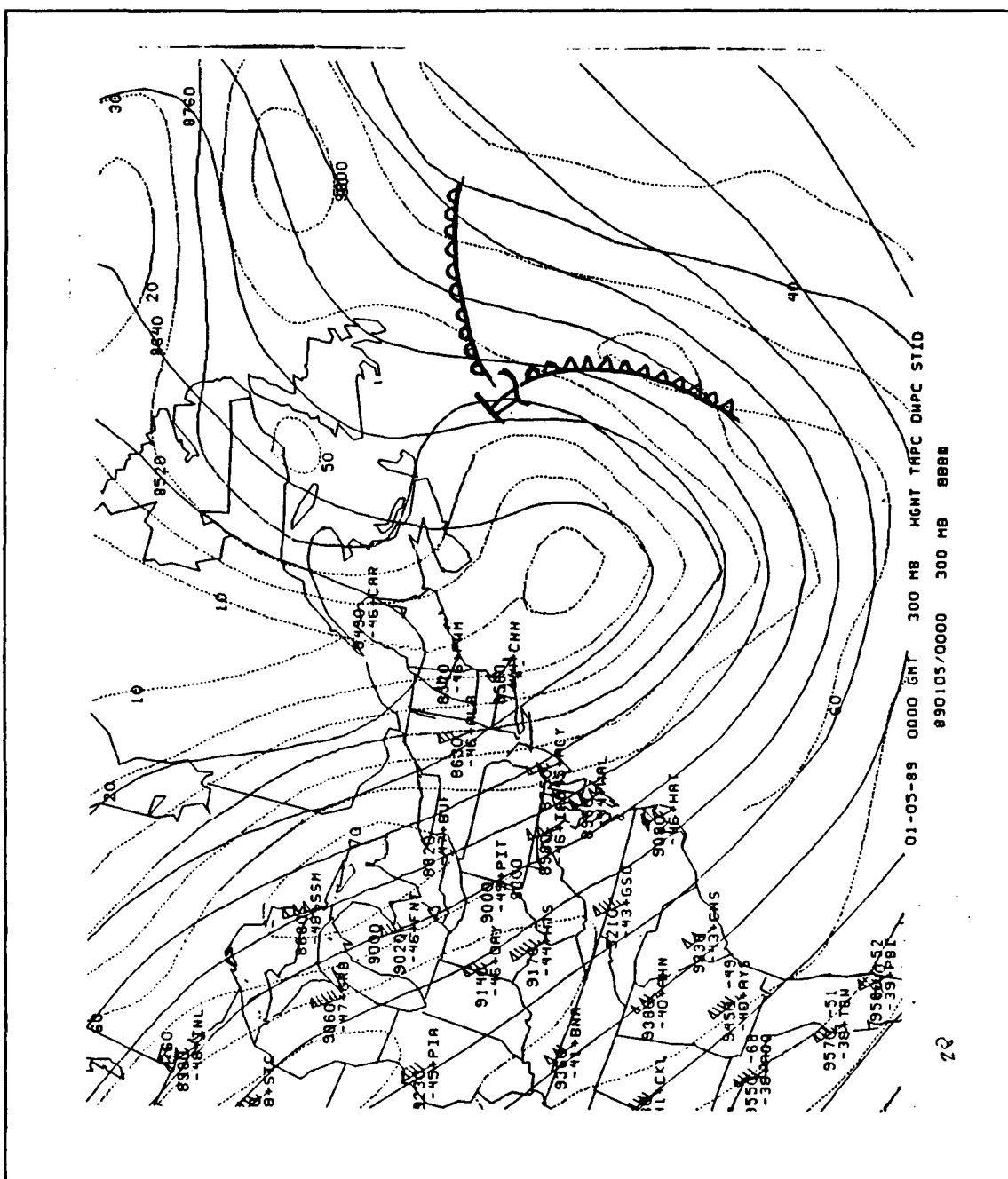


Fig. 28. 0000 UTC 05 January 1989 300 mb Analysis.: Solid lines are geopotential height (m). Dashed lines are isotachs (m/s). Plotted winds are in knots.

IV. COMPARISON OF DYNAMICAL FORCING.

A. UPPER-LEVEL PROCESSES.

As suggested by many other studies [e.g. Sanders (1986), Uccellini et al (1984)], upper-level baroclinic processes are important factors in rapid cyclone development. Both the maritime and continental cyclones in this study had strong upper-level forcing. The land cyclone did not start to rapidly develop until the upper-level forcing was positioned over the surface low. The maritime cyclone formed in response to strong upper-level forcing over the North Carolina coast.

The upper-level forcing for the continental cyclone remained uncoupled from the surface low for about 24 hours. When the upper-level forcing "overran" the surface cyclone, rapid cyclogenesis began to occur. In the maritime case, the upper-level forcing was responsible for the formation of a weak surface low off the Carolina coast. The upper-level forcing was present throughout the development of the maritime cyclone and contributed to explosive development of the cyclone.

During the development of the land cyclone, an upstream entrance-downstream exit dual jet streak pattern formed for this cyclone. The downstream jet developed to the north of the cyclone prior to the cyclone moving into that region. This jet became extremely important because it interacted with the entrance streak to produce large upper-level divergence values. The left side entrance jet exit region and the right side exit jet entrance region were aligned by 0000 UTC 16 November 1988 (Fig. 10). Notice the strong and very localized 300 mb divergence value over Iowa in Fig. 29. Spectral model analysis show a similar evolution of the jet streaks and produced divergence values nearly as large as those in Fig. 29. Within the limits of the 12 h analysis, this time period had the highest values of divergence. The alignment of the jet streak divergence region provided very favorable upper-level divergence over the surface cyclone and rapid development resulted.

The maritime cyclone (03-06 January 1989) was located in the left exit region of a strong jet streak from the onset. The land downstream jet was present before the rapid development stage of the that cyclone and formed in response to confluence with the upstream short wave trough and the downstream ridge. However, a dual entrance-exit configuration does not develop in the ocean case until 1200 UTC 04 January 1989 (within the constraints of 12-hour analysis periods). The downstream exit jet apparently

does not form earlier because the younger cyclone has developed so rapidly that the wavelength is too short between the new cyclone and older cyclone to the northeast. This short wavelength prevents the formation of a downstream ridge and no confluent upper-level flow develops. After the older cyclone propagated to the northeast, a very weak ridge developed (downstream of the developing cyclone) and an exit jet formed by 1200 UTC 04 January 1989 in response to cyclogenesis and warm front baroclinic processes. At this time, the divergence regions of both jets are aligned to enhance upper-level divergence. The 300 mb divergence (Fig. 30.) gives a good depiction of the strong, localized divergence present with these jet streaks. The maritime divergence values are quite similar to the land case values, however, the maritime area of divergence appears to be two to three times as large. This divergence size difference may be a reflection of the different NMC grids used. The ocean case employed the Spectral model with less resolution than the Nested Grid used in the land case. The divergence in the land case also tended to be less concentrated in the Spectral model analysis. Consequently, there may be finer structure in the maritime divergence field that is lost due to resolution of the Spectral model.

There appear to be subtle differences in the upper-level forcing between these continental and maritime cases. Over the land, the cyclone did not become "explosive" until the upper-level divergence caused by both the entrance and exit jet streaks was positioned over the cyclone center. On the other hand, the maritime cyclone was rapidly developing under the forcing of only the entrance jet before the dual jet pattern developed. This difference may only reflect the difference in the upper-level only (land) forcing and the deeper baroclinic forcing in the ocean case. The presence of a jet streak in the upper-level wave provided significant forcing to the surface cyclone in both cases. The shear vorticity generated by the streaks enhanced the curvature vorticity found in the upper trough. The divergence generated by the streaks allowed for increased lower-level convergence, greater vertical motion, and rapid development of the cyclone.

B. SURFACE/LOW LEVEL FORCING.

As is evident in the Petterssen Development equation (Petterssen, 1956), low-level thermal advection plays an equally important role in forcing cyclogenesis. Strong thermal advection greatly enhances the vertical motion in a developing cyclone. In addition, frontogenesis enhances the thermal gradient and jet intensity which results in strong local regions of divergence.

As previously mentioned in the continental cyclone synoptic discussion, there was a $12^{\circ}\text{C}/50\text{ nmi}$ surface temperature difference across the cold front in the early stages of cyclone development. The warm front also displayed a pronounced temperature difference of $10^{\circ}\text{C}/50\text{ nmi}$ during the developing and mature stages of the cyclone. In contrast, the maritime cyclone had much weaker surface temperature differences across the cold and warm front boundaries ($2^{\circ}\text{C}/100\text{ nmi}$ for both fronts) but had significant temperature differences between the warm and cold sectors. It appears that the land cyclone in this study had stronger surface warm and cold fronts. However, the maritime cyclone appears to have greater total baroclinicity as evidenced by comparing the land vertical cross section (Fig. 11) with the ocean vertical cross section (Fig. 22).

The advection of cold air over warm water has a significant impact on cyclogenesis. The sensible heating of the cooler air reduces static stability and aids vertical motions and convection. It is important to examine the heat and moisture fluxes in the boundary layer to gain an insight to the potential affect each may have on cyclogenesis.

Nuss and Kamikawa (1990) examined the interaction of surface heat and moisture fluxes in the boundary layer and their effects on explosive cyclogenesis. By studying the boundary layer equivalent potential temperature budgets, Nuss and Kamikawa were able to separate the increase in equivalent potential temperature into local and advective parts. This study conducted a similar examination, except that the dry potential temperature θ is used. The GEMPAK software available in the Interactive Digital Environmental Lab at the Naval Postgraduate School was utilized for this study. In keeping within the limits of the 12-hour analysis periods and the GEMPAK system, an analysis of the change in θ with time (ultimately heating) was attempted. The time averaged advection of θ by the observed wind (using advection values at the start and end of the 12-h period) was subtracted from the local time derivative of θ to give a residual local change in θ , which represents the contributions of local heating, vertical advection and any errors in the analysis. The local change in θ due to vertical advection was ignored due to its presumed small size at 1000 mb and inaccessibility through the gridded data set and so the residual is assumed to represent primarily surface heating. The major drawback encountered in this calculation was that it is not possible to determine the accuracy of the difference between advection and the time derivative. The equation for calculating θ changes from gridded data uses time averaged θ advection data combined with 12-hour changes in θ and vertical advection is neglected, consequently significant errors are possible. Assuming typical values for the variations of the terms in the thermodynamic equation, it is conceivable that errors are as large as 50 %.

During the early formation of the maritime cyclone over the Virginia-Carolina coast, weak warm advection from the south can be observed. Fig. 31 shows the residual 1000 mb local θ change from 1200 UTC 03 January 1989 to 0000 UTC 04 January 1989. Acknowledging that the error in this analysis method may be as great as 50 %, the above figure shows almost no local heating to the east of the cyclone. It appears that almost all the low level heating resulted from advection. This appears to be consistent with previous observations noted in the synoptic discussions. The cold air has not penetrated south over the water to a great extent during this time frame. There should be little surface heating and large advective changes.

A profile of thermal advection by the geostrophic wind is provided in Fig. 32 for a point about 150 nmi east of the 0000 UTC 04 January 1989 cyclone position. This point was selected as it lies on the track of the cyclone as it developed and propagated to the east. The profile shows warm advection from the surface to 850 mb, then a region of slight cold mid-level advection near 500 mb. This advection pattern reduces the static stability of the air mass ahead of the cyclone in the 850-500 mb layer. It would appear that any effect of surface heating would be to destabilize the layer below 850 mb also.

The next 12 hour period (0000-1200 UTC 04 January 1989) is of particular interest. At 1200 UTC 04 January 1989 the cyclone is located about 300 nmi east of Norfolk. Fig. 33 shows the residual 1000 mb local θ change. Notice the strong local heating in advance of the rapidly developing cyclone.

During the rapid development of the maritime cyclone, the total change in θ is equally divided between advection and local heating. This division of the θ change agrees quite closely to the findings of Nuss and Kamikawa (1990), who also observed a roughly equal split between local heating θ changes and advection.

An advection profile was obtained (Fig. 34) for another point about 100 nmi down the cyclone track. The warm advection decreases from the surface to 700 mb, which again tends to reduce the stability ahead of the surface cyclone.

Similar θ calculations for the land case were attempted. However, the data fields necessary to calculate the θ change were limited to the NMC Spectral model analysis fields for 1200 UTC 15 November 1988 to 0000 UTC 16 November 1988. The results were markedly different from the maritime case. At 1000 mb, almost the entire residual θ change was from advection. There was apparently little or no boundary layer heating associated with this time period. Fig. 35 displays the residual 1000 mb local change in θ . The low values of local θ suggest that there is little local heating occurring with this cyclone.

C. STATIC STABILITY.

As is evident in the Petterssen Development equation (Petterssen 1956), or the omega equation, static stability can greatly modify the response to forcing by vorticity or thermal advection. A low stability environment is favorable for a large response (rapid development). However, the static stability changes with time due to thermal advection and surface heating processes. The stability may not remain favorably low for extended periods of time. Maintenance of a low static stability environment can occur in several ways; low level heating which may be due to the surface heat flux or strong upper level cooling due to cold advection aloft. Nuss (1989), suggests that surface heat flux influences on static stability are confined to the boundary layer. The static stability was generally low during the entire maritime evolution, indicating some mechanism for maintaining this situation (see Figs. 38 and 39). The continental cyclone exhibited strong static stability except for one brief period at the onset of development which indicates little or no mechanism for maintenance.

The static stability for the continental cyclone started at low values and increased with time. At 1200 UTC 15 November 1988, the surface cyclone was located over the Texas-Oklahoma panhandle border. Fig. 36 shows some low stability in the immediate cyclone vicinity. This period is interesting as it was the onset of strong coupling with the upper-level forcing and marked the start of the rapid intensification phase of the storm. After this time period, the land cyclone displayed increased stability along the frontal zones and in the vicinity of the cyclone center. Fig. 37 gives a good example of the high stability encountered at 1200 UTC 16 November 1988. The surface cyclone was located over Lake Superior and was continuing to intensify. Notice the high stability values along the warm and cold frontal zones. Similar values were obtained using the Spectral model analysis for this case so the NGM data are taken as representative. Comparison of θ changes due to advection at 1000 and 500 mb revealed that the low-level warm advection should have reduced the static stability ahead of the cyclone. However, since the static stability increased from 1200 UTC 15 November 1988 to 1200 UTC 16 November 1988, other factors must have offset the low-level advection. Convection and latent heat release coupled with warm advection at the mid-levels may have provided the stabilizing influence.

The maritime static stability was lower than the continental stability. The presence of warm water underlying a cold air mass implies low-level heating, as previously discussed. It is interesting to examine the differences in static stability for a couple of time periods during the maritime storm. Fig. 38 depicts the stability for 0000 UTC 04 January

1989. The overall stability appears to be low near the cyclone center, about 4 units. During the next 24 hours, the stability increases in the vicinity of the cyclone center to about 4.5 units (Fig. 39).

Several factors contribute to the reduction of static stability over the water. As mentioned previously, the boundary layer sensible heating from the warmer surface water destabilizes the boundary layer. The differential advection at mid levels also enhances the instability. The air mass immediately ahead of the cyclone had cold advection at the 700 mb level. This profile is unstable and would support convection quite well. Strong convection was encountered near the cyclone, along the cold front and in the cold air behind the front. However, convection acts to re-stabilize the environment through latent heat distribution and may explain the slowly increasing static stability mentioned previously.

D. SUMMARY.

The continental and maritime cyclones demonstrated some differences in the evolution of the upper-level forcing. The land case developed two strong jets early in the cyclone development, with the downstream jet resulting from upper-level confluence. The ocean case did not develop a dual jet streak until the cyclone was already rapidly developing because of the presence of the older cyclone to the northeast. When the downstream streak did develop, it was in response to cyclogenesis. In both cases, strong embedded jet streaks provided good shear vorticity and greatly enhanced upper-level divergence. It was interesting to note that in both cyclones, a dual entry-exit jet streak pattern develops with optimum positioning of the divergence regions. Additionally, strong positive vorticity advection was available, not only from the curvature in the upper trough, but from shear, generated by the jet streaks. The upper-level forcing in the land case was responsible for the onset of rapid cyclone development. Further, the continental cyclone probably would not have developed in the absence of this forcing. The upper forcing also produced the upper-level divergence that allowed for development of the surface depression that rapidly developed into the intense maritime cyclone.

At the lower levels, there was some discernable differences in the temperature gradient across warm and cold fronts between the land and ocean cases. The land cyclone had very strong temperature gradients while the ocean case had little gradient, spread over a large area. There was some difference in thermal advection between the two cases. Both cases had differential advection. The land case had some strong lower-level warm advection with weaker warm advection at the mid-levels. The oceanic case had

strong low-level warm advection and weak cold advection at the mid-levels. This advection profile proved to be a destabilizing influence on the oceanic air mass. While advection seemed to be the primary mechanism for heating and cooling of the land cyclone, the oceanic case had several instances where the warm southerly advection was significantly enhanced by local heating, probably by the warmer North Atlantic surface water.

Initially the static stability was low for the continental case and rapidly increased during the cyclone development. Low-level warm advection appears to have been countered by mid-level warming from convection and advection. In contrast, the oceanic static stability was universally quite low. The warmer water underlying the cold air produced a continued low-level heat source that was not well balanced by mid-level convection. The maritime environment also appears to maintain low static stability for significant periods of time. Additionally, the differential advection with cooler advection at the mid-layers, also helped to destabilize the air mass. The absence of static stability proved to be a key feature in the explosive development of the maritime storm. Both the land and ocean storms had strong upper-level forcing, yet the oceanic storm developed much faster and to a greater extent. The low static stability of the maritime case allowed for greatly enhanced vertical motion, which in turn, enhances upper-level divergence, allows for deepening of the surface low, provides for increased convection and additional release of latent heat. The extra heating further increases vertical motion, and a strong positive feedback loop is established.

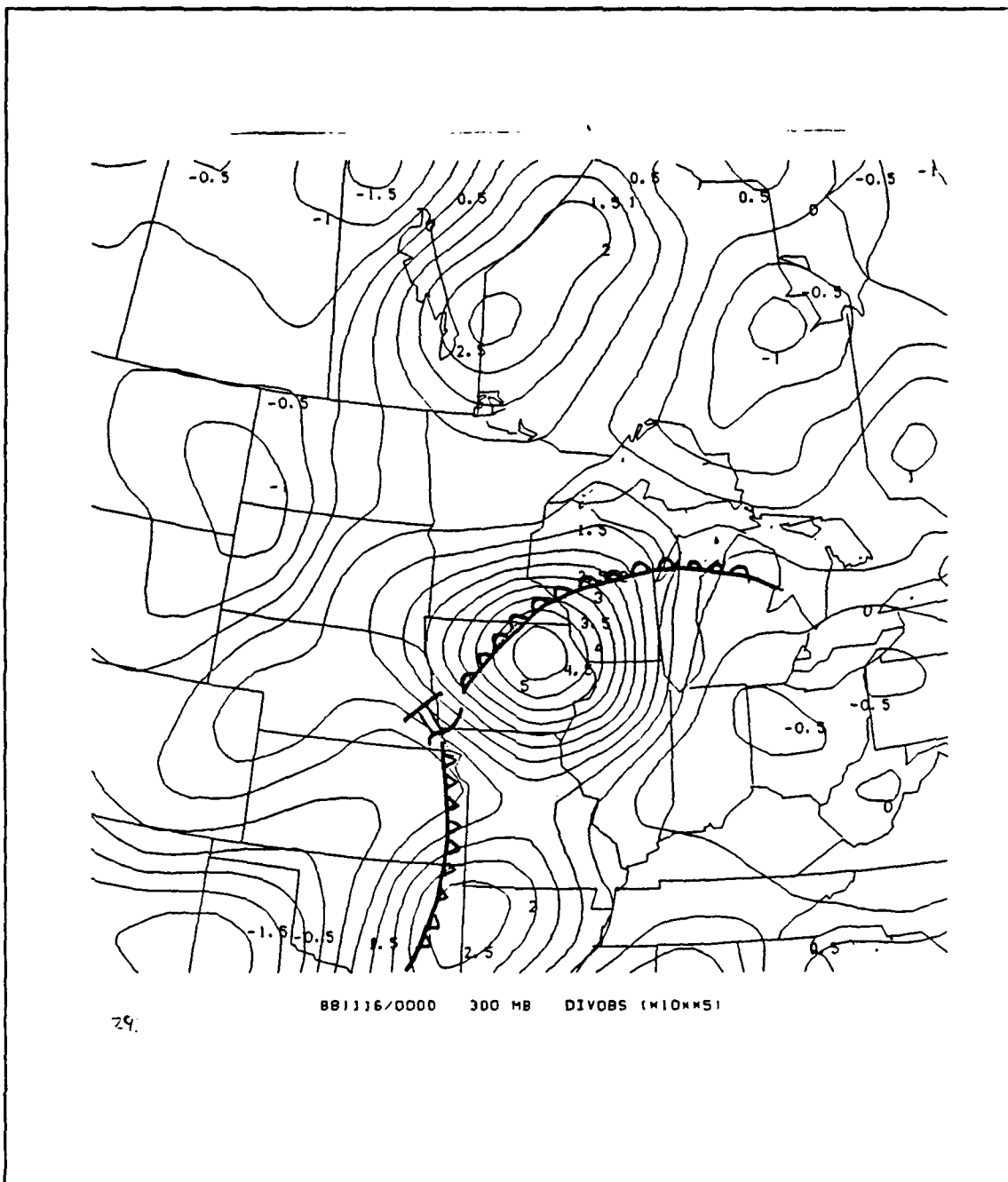


Fig. 29. 0000 UTC 16 November 1988 300 mb Divergence: Solid lines are $10^{-5} s^{-1}$ contours.

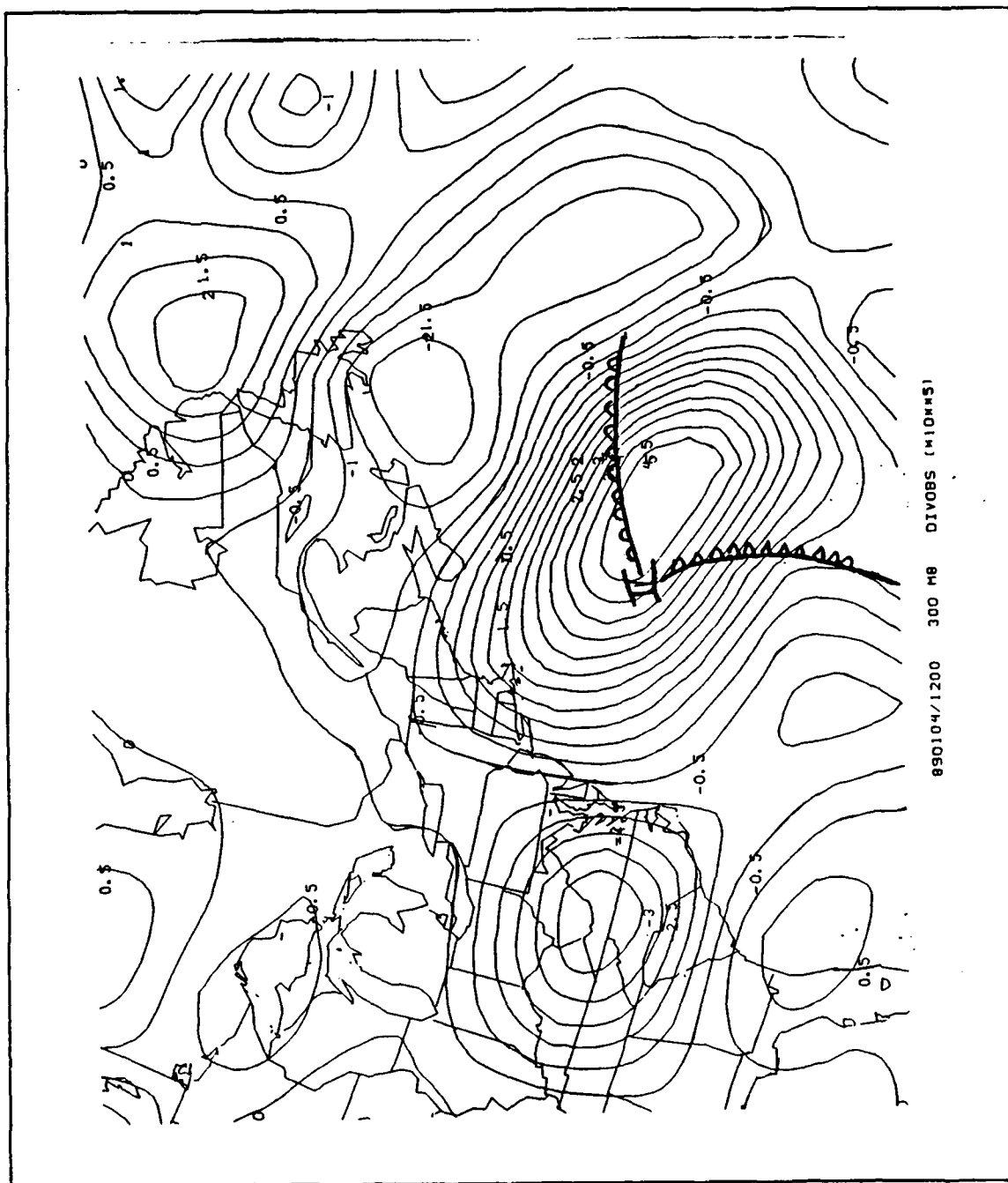


Fig. 30. 1200 UTC 04 January 1989 300 mb Divergence: Solid lines are $10^{-5} s^{-1}$ contours.

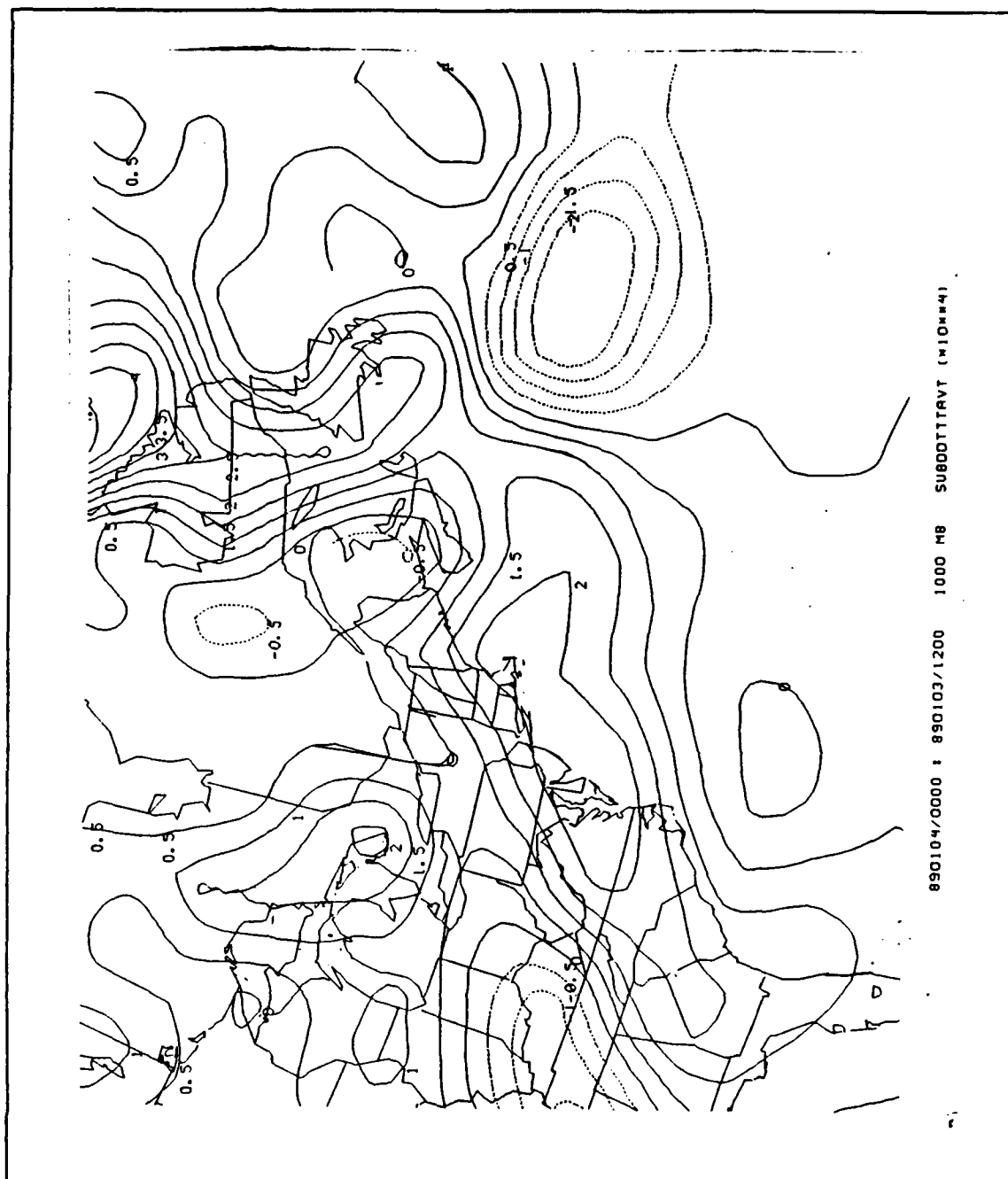
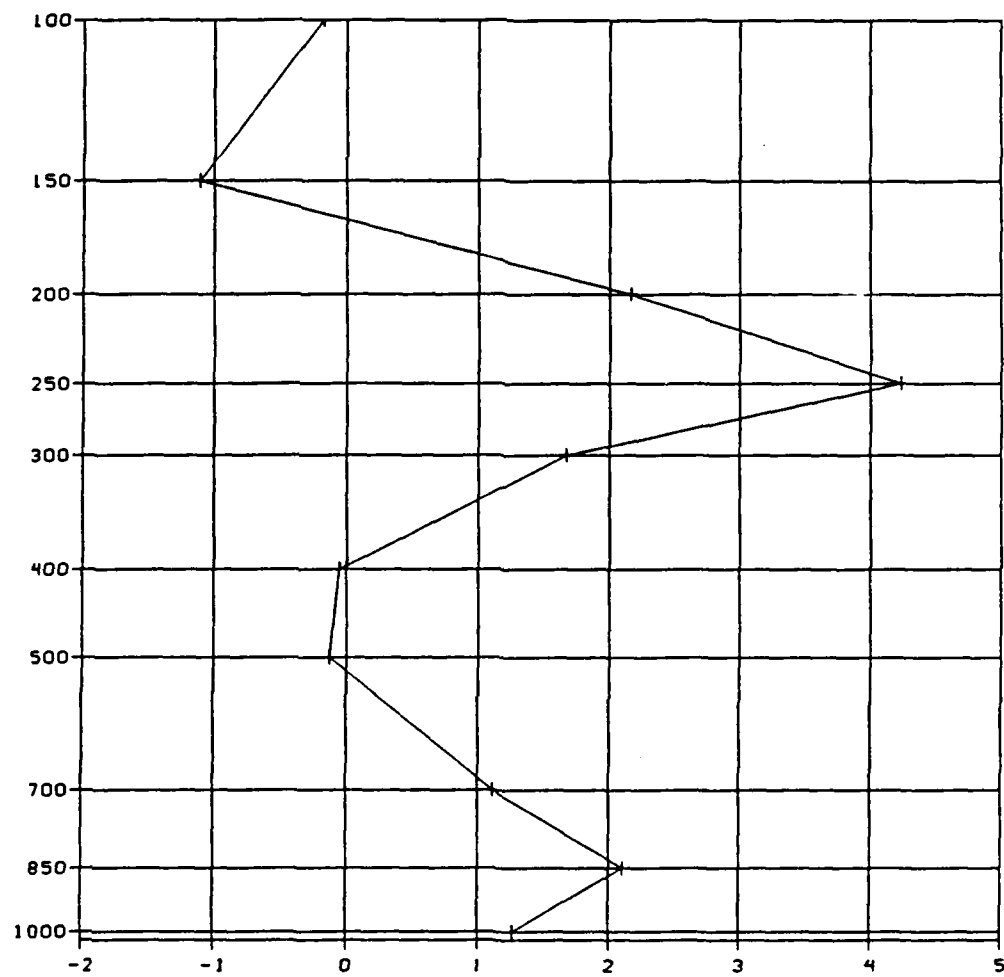


Fig. 31. 1800 UTC 03 January 1989 1000 mb θ Local Change: Solid lines are positive 10^{-4} k/s contours. Dashed lines are negative 10^{-4} k/s contours.



32

890104/000

ADVTHPKGE0 (X10**4)

Fig. 32. 0000 UTC 04 January 1989 Temperature Advection Profile: Advection in 10^{-4} k/s. Profile taken at 35°N , 070°W .

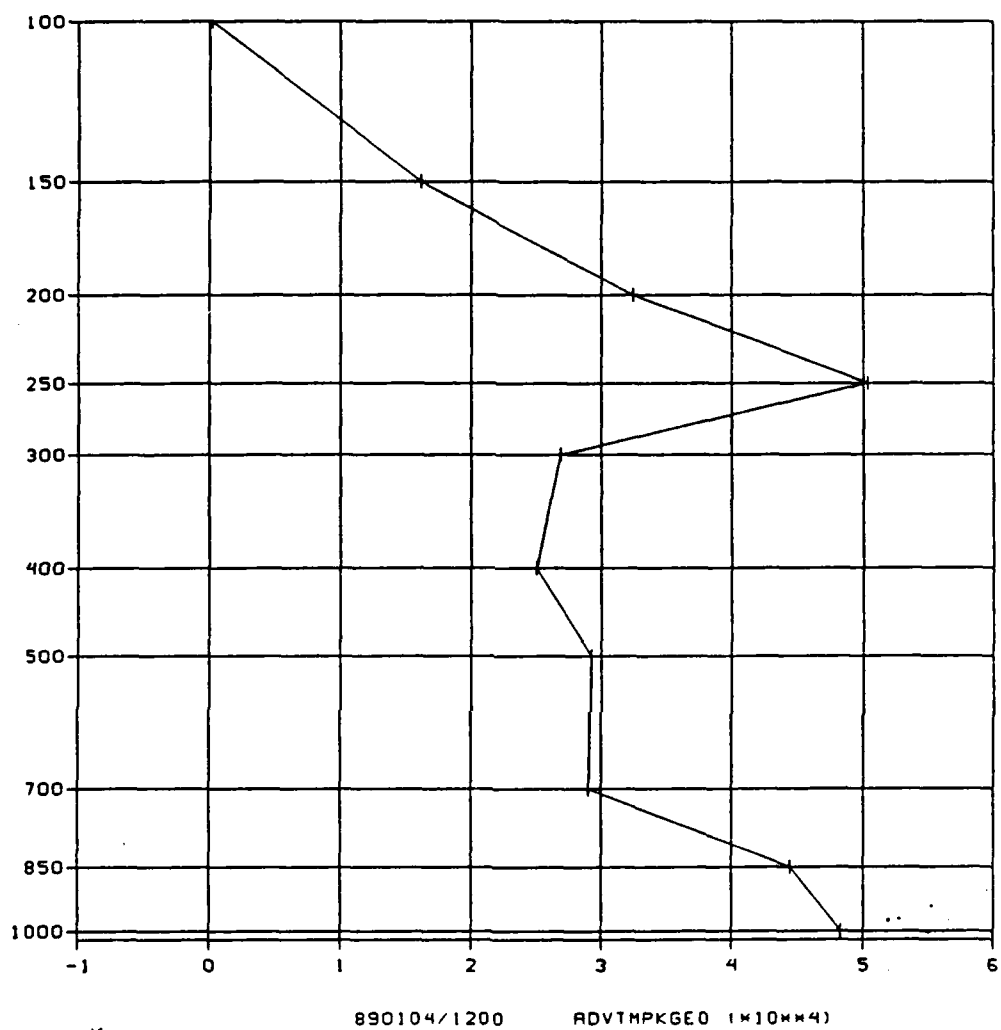


Fig. 34. 1200 UTC 04 January 1989 Temperature Advection Profile: Advection in 10^{-4} k/s. Profile taken at 37°N , 061°W .

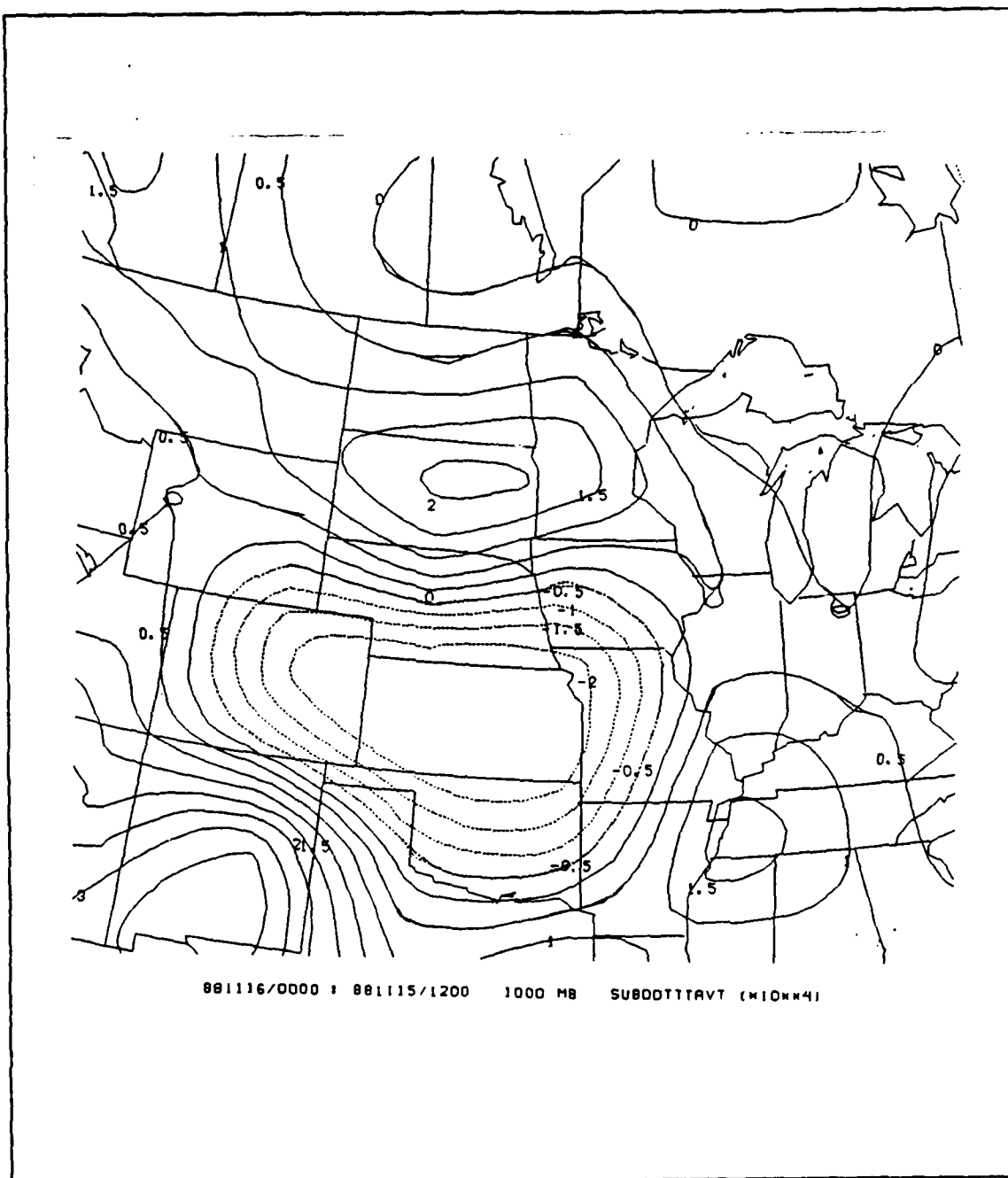


Fig. 35. 1800 UTC 15 November 1988 1000 mb θ Local Change: Solid lines are positive 10^{-4} k/s contours. Dashed lines are negative 10^{-4} k/s contours.

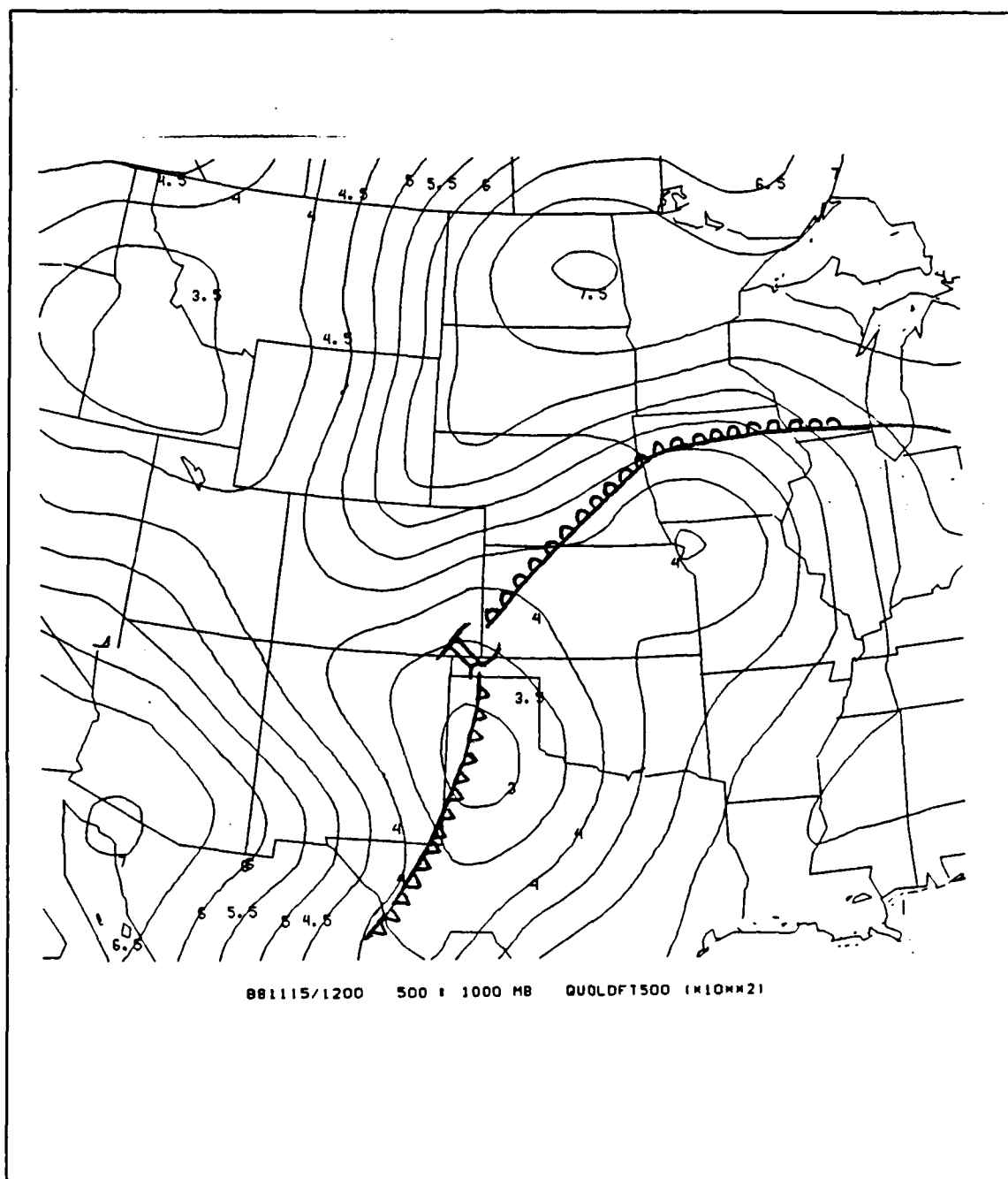


Fig. 36. 1200 UTC 15 November 1988 Static Stability: Solid lines are 10^{-2} K/mb contours.

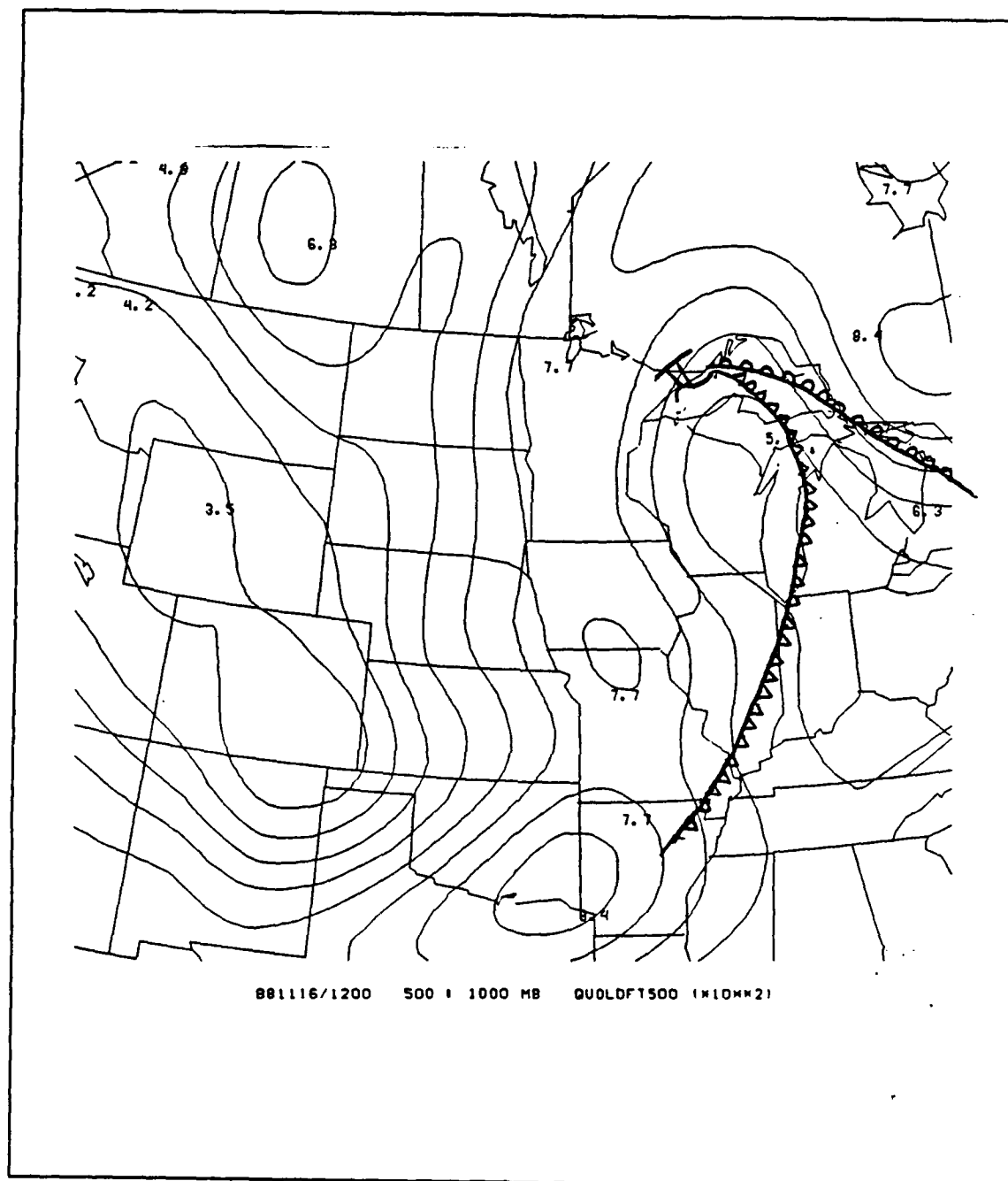


Fig. 37. 1200 UTC 16 November 1988 Static Stability: Solid lines are 10^{-2} K/mb contours.

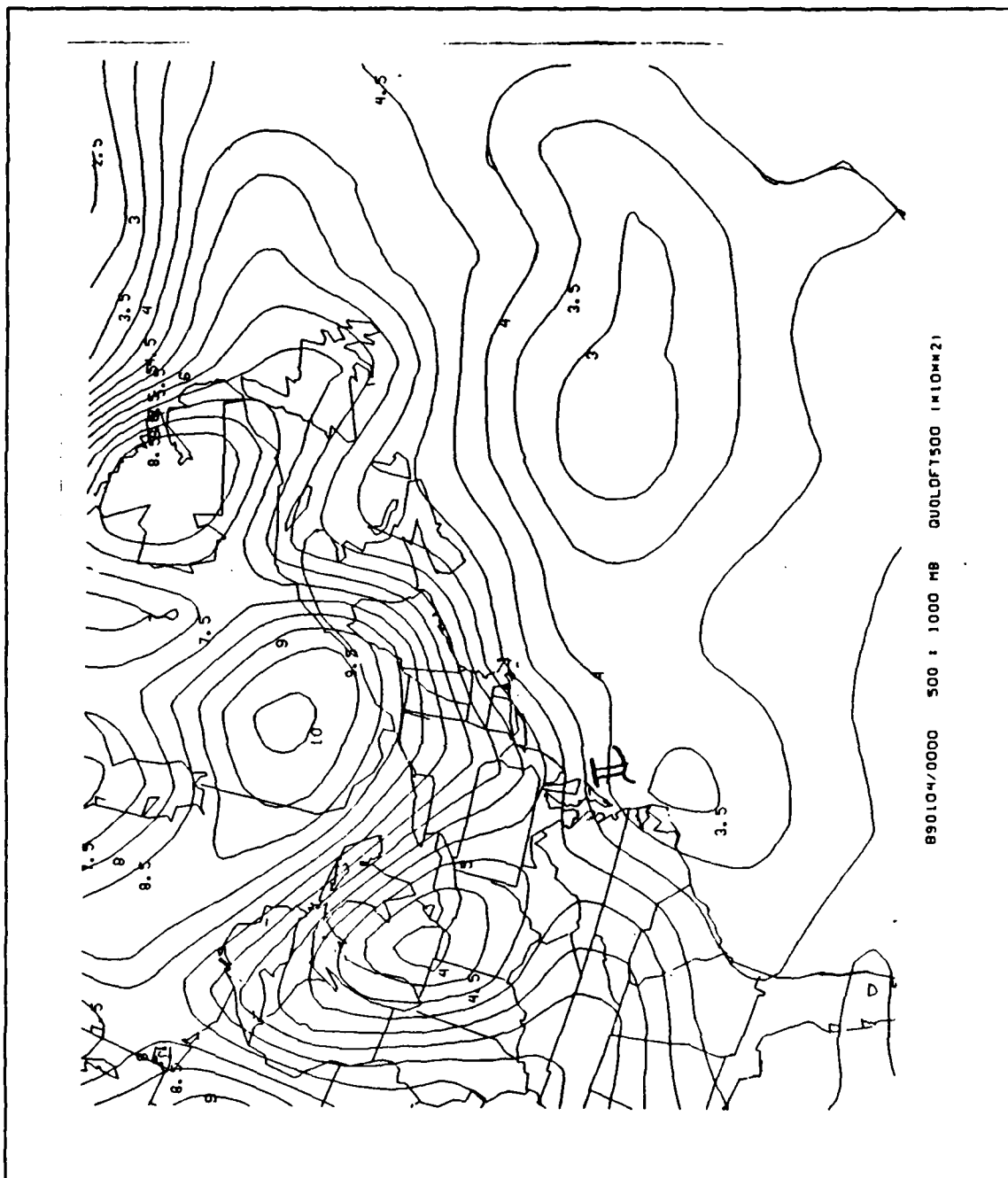


Fig. 38. 0000 UTC 04 January 1989 Static Stability: Solid lines are 10^{-2} K/mb contours.

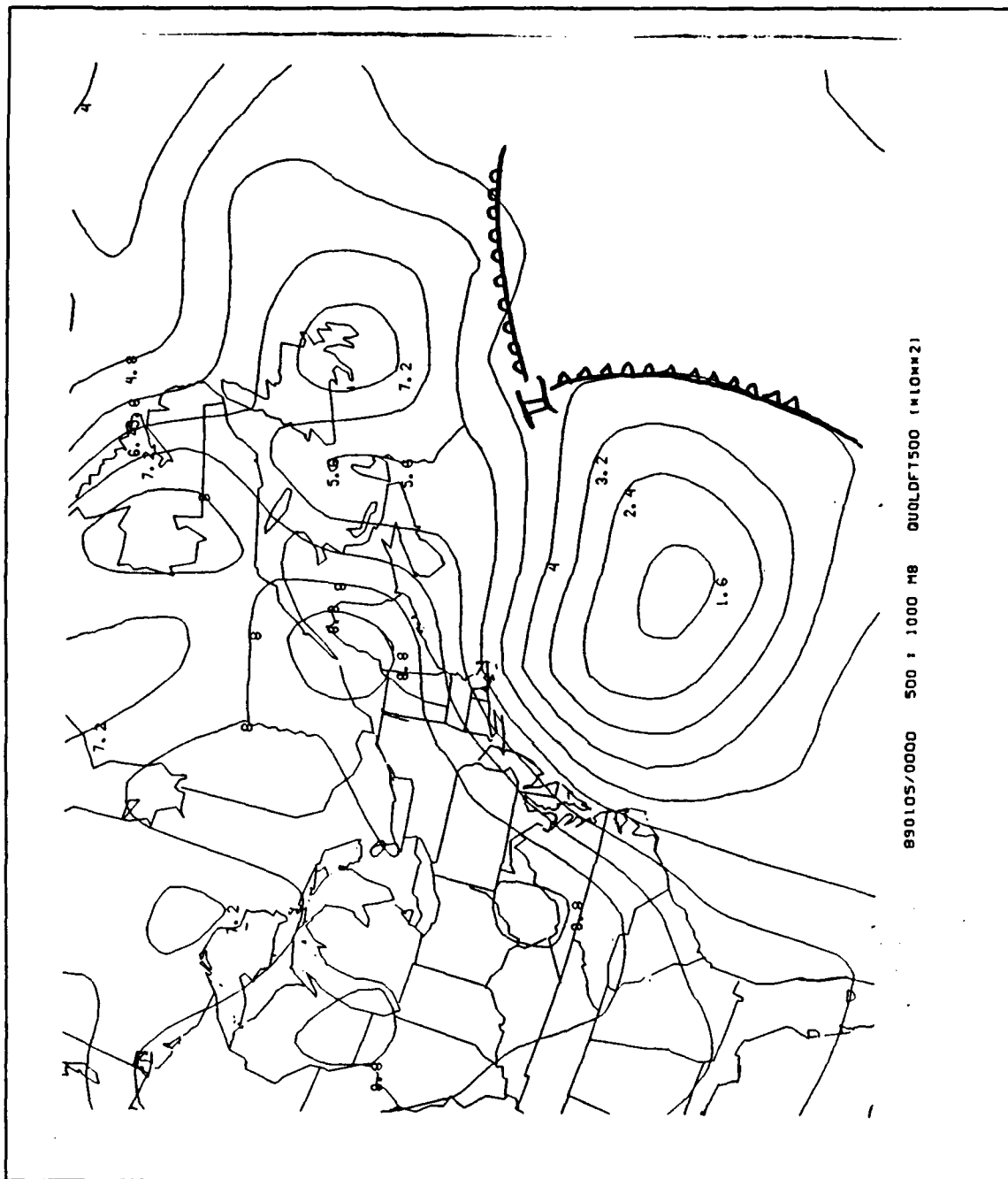


Fig. 39. 0000 UTC 05 January 1989 Static Stability: Solid lines are 10^{-2} K/mb contours.

V. CONCLUSIONS.

The analysis of a rapidly developing land and oceanic cyclone has shown that:

1. The upper-level forcing of the two cyclones appears to be quite similar during the mature stage of development. In particular, a dual entrance-exit jet configuration was observed for both cyclones. This dual jet structure evolved from quite different initial configurations. In the land cyclone, the dual jet streaks formed early and the downstream jet formed in response to confluence at upper-levels. The maritime dual jet pattern formed relatively late with the downstream streak forming in response to cyclogenesis and strong baroclinic warm front processes.

2. When the left side exit region of the upstream streak and the right side entrance region of the downstream jet are aligned, maximum upper-level divergence and surface development are observed. In the land case, this strong divergence results from the interaction of two pre-existing jet streaks. In the ocean case, strong divergence already existed due to the strong upstream jet. As baroclinic processes of the warm front developed the downstream jet, divergence over the surface cyclone was further enhanced.

3. Although both cyclones displayed strong low-level thermal advection, the processes that created this strong advection are different. At 1000 mb, the total change in potential temperature θ is mostly from advection for the land case. Over the water, the 1000 mb θ change appears to be divided between advection and local boundary layer heating. This indicates an active role of the surface heat fluxes in the oceanic cyclone.

4. Initially, both cyclones had low static stability. However, the static stability evolved very differently in the continental and maritime cyclones. Over the land, static stability increased due to convection and weak warm advection at mid-levels, especially in the vicinity of the frontal zones of the cyclone. In contrast, static stability remained low in the oceanic cyclone due to strong surface heating and cold advection at the upper-levels.

The oceanic cyclone developed much more rapidly and to a far greater extent than did the land cyclone. Assuming equal contribution by the similar upper-level forcings (nearly equal divergence values) in these cases, the difference in cyclone intensity must be attributed to low-level processes and static stability differences. Some specific recommendations for further study include: 1). Detailed analysis of the ocean case using ERICA data to better resolve jet streak warm front interaction. 2). A surface

flux planetary boundary layer analysis to provide more definite evaluation of the surface heating contribution in the ocean cyclone. 3). Detailed analysis of the jet interaction in the land cyclone, possibly through model studies. 4). Complete analysis of the static stability evolution in both cases to better understand why low static stability is maintained in the oceanic case and not the land case.

LIST OF REFERENCES

- Bosart, L. F. and S. C. Lin, 1984: A diagnostic analysis of the Presidents' Day storm of February 1979. *Mon. Wea. Rev.*, **112**, 2148-2177.
- Kocin, P. J., and L. W. Uccellini, 1985: A survey of major East Coast snowstorms, 1960-1983. Part 1: Summary of surface and upper-level characteristics. *NASA Technical Memorandum 86196*, NASA, Goddard Space Flight Center, Greenbelt MD, 20771.
- Nuss, W. A., 1989: Air-sea interaction influences on the structure and intensification of an idealized marine cyclone. *Mon. Wea. Rev.*, **117**, 351-369.
- , and S. I. Kamikawa, 1990: Dynamics and boundary layer processes in two Asian Cyclones. *Mon. Wea. Rev.*, In Press.
- Palmen, E., and C. W. Newton, 1969: *Atmospheric Circulation Systems*. Academic Press, 603 pp.
- Petterssen, S., 1956: *Weather Analysis and Forecasting, Vol. 1*. McGraw-Hill, 428 pp.
- Reed, R. J. and M. D. Albright, 1986: A case study of explosive cyclogenesis in the eastern Pacific. *Mon. Wea. Rev.*, **114**, 2297-2319.
- Roebber, P. J., 1984: Statistical analysis and updated climatology of explosive cyclones. *Mon. Wea. Rev.*, **112**, 1577-1589.
- Sanders, F., 1986: Explosive cyclogenesis in the west central North Atlantic ocean, 1981-1984. Part 1: Composite structure and mean behaviour. *Mon. Wea. Rev.*, **114**, 1781-1794.
- , 1989: *A series of surface maps for ERICA IOP #1-#5*. July 1989, Marblehead, MA, 01945.

-----, and J. R. Gyakum, 1980: Synoptic dynamic climatology of the bomb. *Mon. Wea. Rev.*, **108**, 1589-1606.

Uccellini, L. W., P. J. Kocin, R. A. Petersen, C. H. Wash, and K. F. Brill, 1984: The Presidents' Day cyclone of 18-19 February 1979: Synoptic overview and analysis of the subtropical jet streak influencing the pre-cyclogenetic period. *Mon. Wea. Rev.*, **112**, 31-55.

-----, R. A. Petersen, K. F. Brill, P. J. Kocin, and J. J. Tuccillo, 1987: Synergistic interactions between upper-level jet streak and diabatic processes that influence the development of a low-level jet and a secondary coastal cyclone. *Mon. Wea. Rev.*, **115**, 2227-2261.

INITIAL DISTRIBUTION LIST

		No. Copies
1.	Defense Technical Information Center Cameron Station Alexandria, VA 22304-6145	2
2.	Library, Code 0142 Naval Postgraduate School Monterey, CA 93943-5002	2
3.	Chairman (Code 63Rd) Department of Meteorology Naval Postgraduate School Monterey, CA 93943-5000	1
4.	Chairman (Code 68Co) Department of Oceanography Naval Postgraduate School Monterey, CA 93943-5000	1
5.	Professor Wendell A. Nuss (Code 63Nu) Department of Meteorology Naval Postgraduate School Monterey, CA 93943-5000	2
6.	Professor Carlyle H. Wash (Code 63Wa) Department of Meteorology Naval Postgraduate School Monterey, CA 93943-5000	1
7.	LCDR. Michael E. Kreyenhagen, USN COMCRUDESGRU 2 FPO Miami, FL 34099-4701	2
8.	Director Naval Oceanography Division Naval Observatory 34th and Massachusetts Avenue NW Washington, DC 20390	1
9.	Commander Naval Oceanography Command Stennis Space Center, MS 39529-5000	1
10.	Commanding Officer Naval Oceanographic Office Stennis Space Center, MS 39522-5001	1

- | | | |
|-----|--|---|
| 11. | Commanding Officer
Fleet Numerical Oceanography Center
Monterey, CA 93943 | 1 |
| 12. | Commanding Officer
Naval Oceanographic and Atmospheric Research Laboratory
Stennis Space Center, MS 39522-5005 | 1 |
| 13. | Commanding Officer
Naval Oceanographic and Atmospheric Research Laboratory
Monterey, CA 93943-5006 | 1 |
| 14. | Chairman, Oceanography Department
U.S. Naval Academy
Annapolis, MD 21402 | 1 |
| 15. | Chief of Naval Research
800 North Quincy Street
Arlington, VA 22217 | 1 |
| 16. | Office of Naval Research (Code 420)
Naval Ocean Research and Development Activity
800 North Quincy Street
Arlington, VA 22217 | 1 |
| 17. | Library Acquisitions
National Center for Atmospheric Research
P.O. Box 3000
Boulder, CO 80307 | 1 |